

5-5 Relationship between Diamond Drilling Results and Geological Survey Results

(1) Altered porphyritic granite (Pg1)

Porphyritic granodiorite is classified into altered porphyritic granite (Pg1) and unaltered porphyritic granite (Pg2) by differences in mode of alteration. Porphyry copper type mineralization is embedded Pg1 in the Guzelyayla Area. The intrusion was inferred to be vertical in form, since it could not be unravelled by the initial phase geological survey. The drilling survey of the second and third phases revealed that Pg1 had intruded into andesite of the Zigana Formation. It dips 60° to 70° south-east. Alteration zoning indicates that the center of mineralization is situated slightly east of the intrusion. Investigation of fluid inclusions also reveals that the homogenization temperature of the inclusions is higher and boiling phenomena of the inclusions is observed in samples collected from the Mat Dere to Hasan Dere area. This also is in accord with the above conclusion.

Most ore minerals were leached and limonitized on the surface, and primary sulphide ore, especially chalcopyrite and molybdenite, were recognizable only at Hasandere. As mentioned earlier, ore minerals in the high ridge area were almost completely leached. Only unleached molybdenites remained. Drilling results of MJT-3, 7 and 8 indicate that Cu ore minerals were leached from the surface of the projected ridge in the altered porphyritic granite area, but the zone below remains the primary ore zone. A secondary enrichment ore zone is intercalated between the leached and primary zones.

(2) Andesite (Zigana Formation)

In the andesite of the Zigana Formation-distributed in an area from MJT-1 and 2 sites to the MJT-8 site upstream of Mat Dere and surrounding altered porphyritic granite (Pg1)- a magnetite-pyrite bearing zone (chalcopyrite may be leached) is observed. Andesites of MJT-1, 2 and 8 contain as much magnetite as the surface rock, and surround Pg1. The part having extensive distribution of the propylitic zone (chlorite-magnetite-pyrite) is regarded as the marginal part of mineralization, regardless of strong or weak mineralization. On the basis of this fact, the prospectable area is 1.8 km × 1.8 km covering the andesite and Pg1 areas.

(3) Ore Minerals

Sulphide ore minerals occur in the following areas ;

- ① Magnetite: It is distributed as veins and disseminations in the propylitic zone, and is accompanied by a small amount of

hematite.

- ② Pyrite: It occurs along fissures in quartz veins and as disseminations throughout the mineralized area, but especially in the propylitic zone to the phyllic zone.
- ③ Chalcopyrite: Distribution extends from the potassic zone to the propylitic zone. The mineral assemblage is mainly chalcopyrite-pyrite in fissures, and chalcopyrite-pyrite-quartz in quartz veins. Chalcopyrite content increases toward the center of the mineralization.
- ④ Molybdenite: It is distributed over the potassic zone to the propylitic zone. Molybdenite assemblages are mostly quartz-molybdenite, and quartz-pyrite-molybdenite.
- ⑤ Sphalerite: Some sphalerite is observed in the potassic zone of MJT-3.
- ⑥ Chalcocite, covellite and native copper:
They are present in the secondary enrichment zone of the phyllic zones of MJT-3, 5, 7 and 8.

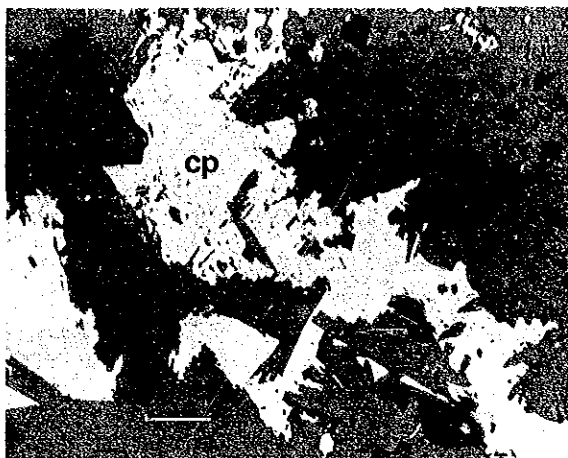
(4) Geological structure

Porphyry copper type ore deposits generally accompany stock-formed intrusive rock. Such intrusives usually intrude along tectonic lines of weakness such as faults and lineaments. Rocks and formations in the area have commonly been displaced by fault movements along tectonic lines. This area was investigated from this point of view, and a survey inferred, post-mineralization fault striking north-south was found by this geological survey. Unaltered porphyritic granite (Pg2) extends in an east-west direction, and altered porphyritic granite (Pg1) may be distributed to the southwest~northeast direction. These intrusions may have intruded along the latest tectonic lines.

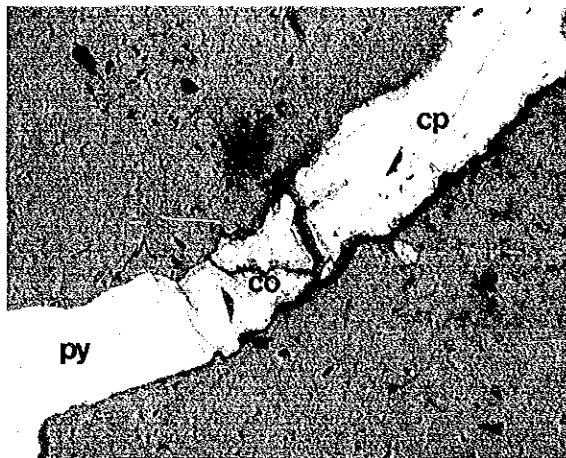
(5) Mineralization

Mineralization is in the form of disseminations, veinlets and fissures. In the center of the potassic zone, chalcopyrites and molybdenites are mainly embedded along fissures, but mineralization is weak. In the phyllic zone of the periphery of the core (potassic zone), chalcopyrites and molybdenites occur not only in fissures and quartz veins but also as disseminations in Pg1, so mineralization becomes strong. This is also the case for the phyllic zone of MJT-3, which is close to the core. Mineralization in MJT-1, 2 and 8 mainly is accompanied with quartz veins in the propylitic zone. Characteristics of mineralization in each hole are as follows;

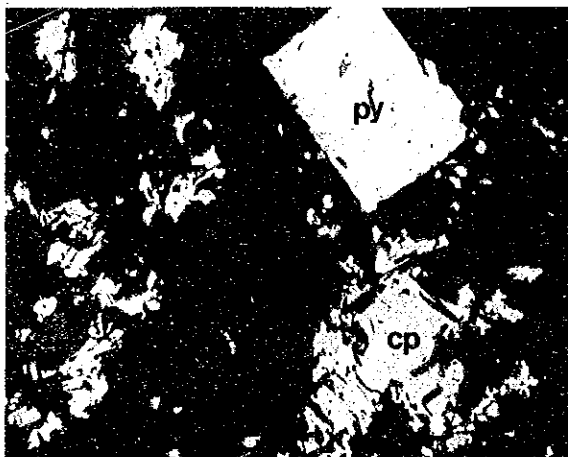
Cp Ore (MJT-4:50.3m)



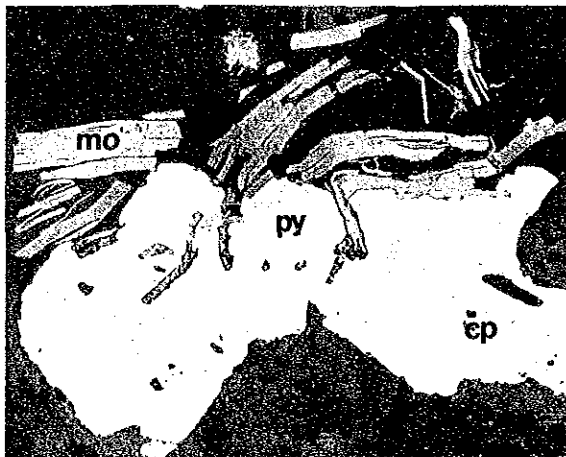
Cp-Cc Ore (MJT-5:49.0m)



Cp Ore (MJT-5:89.3m)



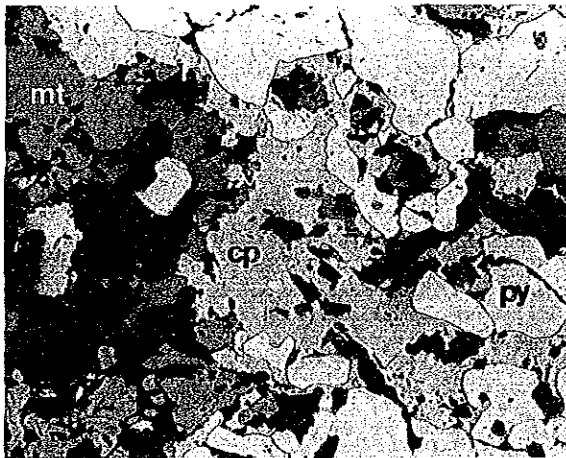
Cp-Mo Ore (MJT-6:66.2m)



Cc-Cp Ore (MJT-7:10.4m)



Cp-Mt Ore (MJT-8:277.4m)

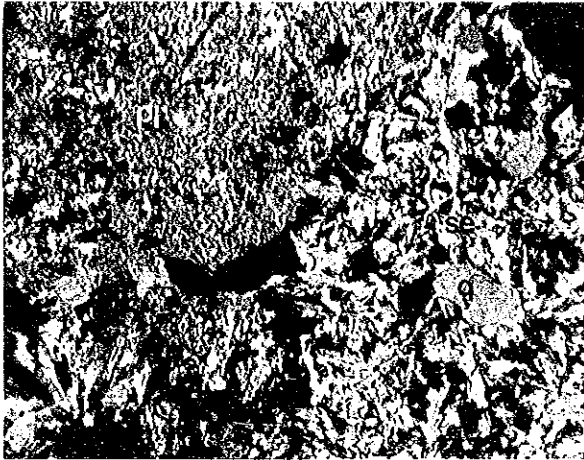


mo:molybdenite cc:chalcocite co:covellite
cp:chalcopyrite mt:magnetite py:pyrite

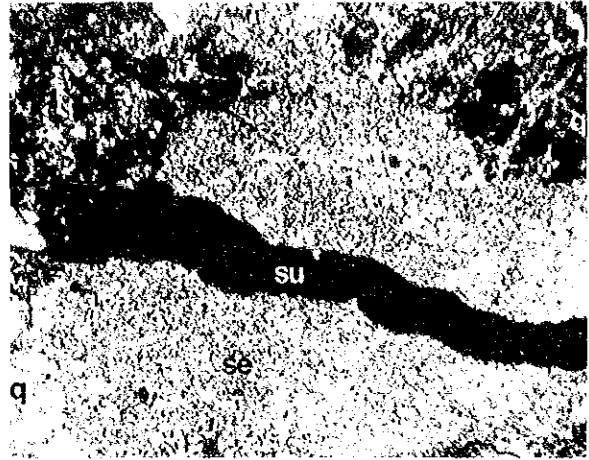


Photograph Microscopic Photographs (No 1)

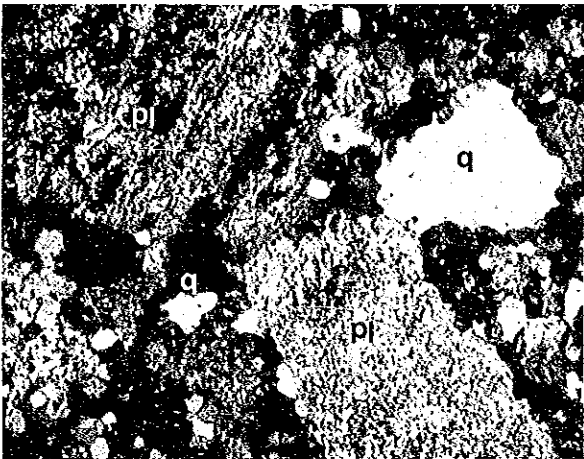
Biotite Pgl (MJT-4:253m)



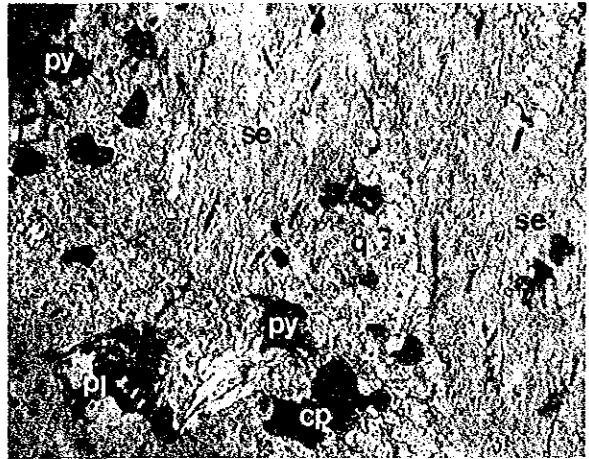
Biotite Pgl (MJT-5:49.0m)



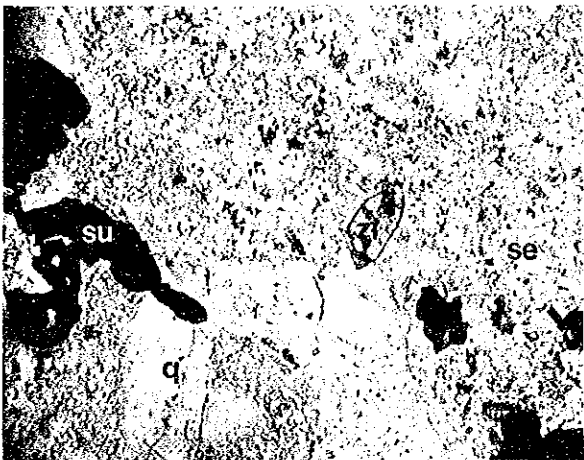
Biotite Pgl (MJT-6:20.0m)



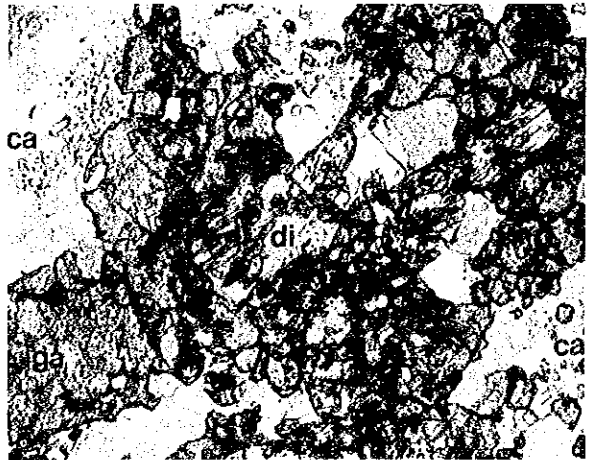
Pgl (MJT-8:27.0m)



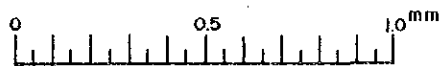
Granodiorite (MJT-9:183.8m)



Skarn (MJT-10:105.9m)



pl:plagioclase q:quartz se:sericite zi:zircon ca:calcite
 ga:garnet di:diopside py:pyrite cp:chalcopyrite
 op:opaque minerals su:sulphide minerals



Photograph Microscopic Photographs (No 2)

Table 21 List of Microscopic Observations of Ore Polished Specimens

No.	Ore	Cp	Co	Cc	Mo	Py	Mt	Ti	He	Qz	Af	Pl	Bi	Se	Ch	Ep	Ca	Gy	Ah	Ka	Ho	
MJT-4	Cu ore (47.9m)	□				△		□														
	Cu ore (50.3m)	□		△		□		□														
	Mo-Cu ore (52.8m)	△		△		□		□														
	Cu-Mo ore (257.8m)	□		□		□		□		⊙												
MJT-5	Cu ore (46.5m)※	□		△		□		△		⊙					□							
	Cu ore (49.0m)※	□		△		□		△		⊙					□							
	Cu ore (89.3m)※	□		△		□		△		⊙					□							
	Cu ore (226.2m)※	□		△		□		△		⊙					□							○
MJT-6	Mo-Cu ore (54.5m)	□				□		□														
	Mo-Cu ore (66.2m)	□				□		□														
	Mo-Cu ore (97.0m)	□				□		□														
	Cu-Mo ore (105.4m)	△				□		□														
MJT-7	Cu ore (7.0m)	○				□		□														
	Cu ore (10.4m)	□		△		□		□														
	Mo-Cu ore (105.0m)	□				□		□														
	Mo-Cu ore (223.2m)	□				□		□														
MJT-8	Mo-Cu ore (263.5m)	△				□		□														
	Cu-Mo ore (298.5m)※	△				□		□		⊙					□							
	Mo-Cu ore (14.6m)※	□				□		□		⊙					□							
	Cu ore (24.0m)	□				□		□		⊙					□							
MJT-9	Cu ore (27.0m)※	□				□		□		⊙					□							
	Mo-Cu ore (56.7m)	○				□		□		⊙					□							
	Cu-Mo ore (131.0m)	□				□		□		⊙					□							
	Cu ore (226.8m)※	□				□		□		⊙					□							
MJT-9	Cu ore (240.0m)※	□				□		□		⊙					□							
	Cu ore (274.7m)	□				□		□		⊙					□							
	Mo-Cu ore (290.0m)	□				□		□		⊙					□							
	Fe ore (183.8m)※	△				□		□		○					□							□?
Fe ore (273.5m)※	△				□		□		○					□							□?	

Cp:Chalcopyrite Co:Covellite Cc:Chalcocite Mo:Molybdenite Py:Pyrite Mt:Magnetite Ti:Ti-Fe mineral
 He:Hematite Qz:Quartz Af:Alk-feldspar Pl:Plagioclase Bi:Biotite Se:Sericite Ch:Chlorite
 Ep:Epidote Ca:Calcite Gy:Gypsum Ah:Anhydrite Ka:Kaoline Ho:Hornblende
 ⊙:Abundant ○:Common □:Few △:Rare ※:Polished-thin section

Drilling No.	Dissemination	Quartz veins	Fissures
MJT-4	△	△	△
MJT-5	△	□	□
MJT-6	□	△	○
MJT-7	△	○	△
MJT-8	□	○	□

○ : common □ : few △ : rare

(6) Alteration Zoning

Zoning of alteration in this surveyed area is characterized by X-ray diffraction analysis as follows;

① Potassic zone: The zone is usually in the core of the porphyry copper type ore deposit, and biotite and potassic feldspar indicate the alteration mode. The zone of the surveyed area is characterized by the existence of a small amount of biotite and potassic feldspar, and additionally contains quartz and anhydrite.

② Phyllic zone: This zone consists of quartz and sericite with a small amount of chlorite as the altered mineral, and surrounds the potassic zone.

③ Argillic zone: This zone is usually distributed at the periphery of the phyllic zone of the porphyry copper type ore deposit, and is represented by kaolinite and montmorillonite minerals, but this zone is absent in the surveyed area.

④ Propylitic zone: The zone containing chlorite, epidote and magnetite is located in the marginal section of alteration in the area.

(7) Fractures in the Mineralized Area

According to the drilling results from MJT-1 to MJT-8, most fractures and shatter cracks have been formed in irregular directions with less than 60° dip. Vertical dip is extremely rare. Detailed survey could not determine a predominant or special direction among the fissures. Furthermore, core collected from 91.2m to 152 m of MJT-1, from 30m to 125m of MJT-3 and from 25m to 254m of MJT-8 were broken into thin plate fragments owing to ribbon structure. Chalcopyrites and pyrites were found along these fractures. Although core recovery was quite low, ore grade of this section generally was good.

5-6 Potentiality of Mineralized Zone

As a result of the drilling surveys in the second and third phases (8 holes 2,508m in total length), the promising mineralized zones were intercepted by drill holes (MJT-3, 6 and 8). Geological ore reserves calculated as more than 0.200% cumulative copper grade are as follows;

	Depth(m)	Cu %	Mo %	Cu+10× Mo%	Reserves(10 ⁶ tones)
MJT-3	0~ 285	0.200	0.009	0.290	200m× 200m× 2.5× 285m=28.8
MJT-6	156	0.277	0.021	0.487	200m× 200m× 2.5× 156m=15.6
MJT-8	0~ 54	0.228	0.010	0.328	200m× 200m× 2.5× 54m= 5.4
Average grade		0.227	0.013	0.356	Total 49.8

The following conditions were applied for calculation:

- ① Ore reserves included the leached zone from surface to 12m of MJT-3 , intrusive rock (Pg2) from 45m to 53m of MJT-6, and the leached zone accompanied by molybdenum from surface to 9m of MJT-8.
- ② Intrusive rock (Pg2) from 111m to 244m was excepted from calculation.
- ③ Size of the polygon of the area was 200m × 200m because the intervals between the drill holes were 200m.
- ④ Gravity equals 2.5.

Geological ore reserves included the predominantly molybdenum mineralized zones of MJT-7 and the lower part of MJT-8 as follows;

	Depth(m)	Cu %	Mo %	Cu+10× Mo%	Reserves(10 ⁶ tones)
MJT-3	0~ 285	0.200	0.009	0.290	200m× 200m× 2.5× 285m=28.8
MJT-6	156	0.277	0.021	0.487	200m× 200m× 2.5× 156m=15.6
MJT-7	0~ 300	0.120	0.013	0.247	200m× 200m× 2.5× 300m=30.0
MJT-8	0~ 300	0.160	0.010	0.264	200m× 200m× 2.5× 300m=30.0
計		0.177	0.012	0.300	104.4

5-7 Relationship between Geophysical Anomaly and Mineralization

Results of the drilling survey and geophysical survey (IP and SIP methods) revealed their relation as follows;

Results of SIP method (second phase)

- ① A zone consisting of high PFE and high phase values was found on survey Line A connecting MJT-1 and MJT-2 holes along Mat Dere. By the SIP survey on the survey Line connecting MJT-2 and MJT-3 holes, the western side of the inferred fault striking north-south has low PFE and low phase value. The part between MJT-2 and MJT-3 sites has a somewhat high PFE

GEOLOGICAL PROFILES OF GÜZELYAYLA AREA (MAÇKA - TRABZON)

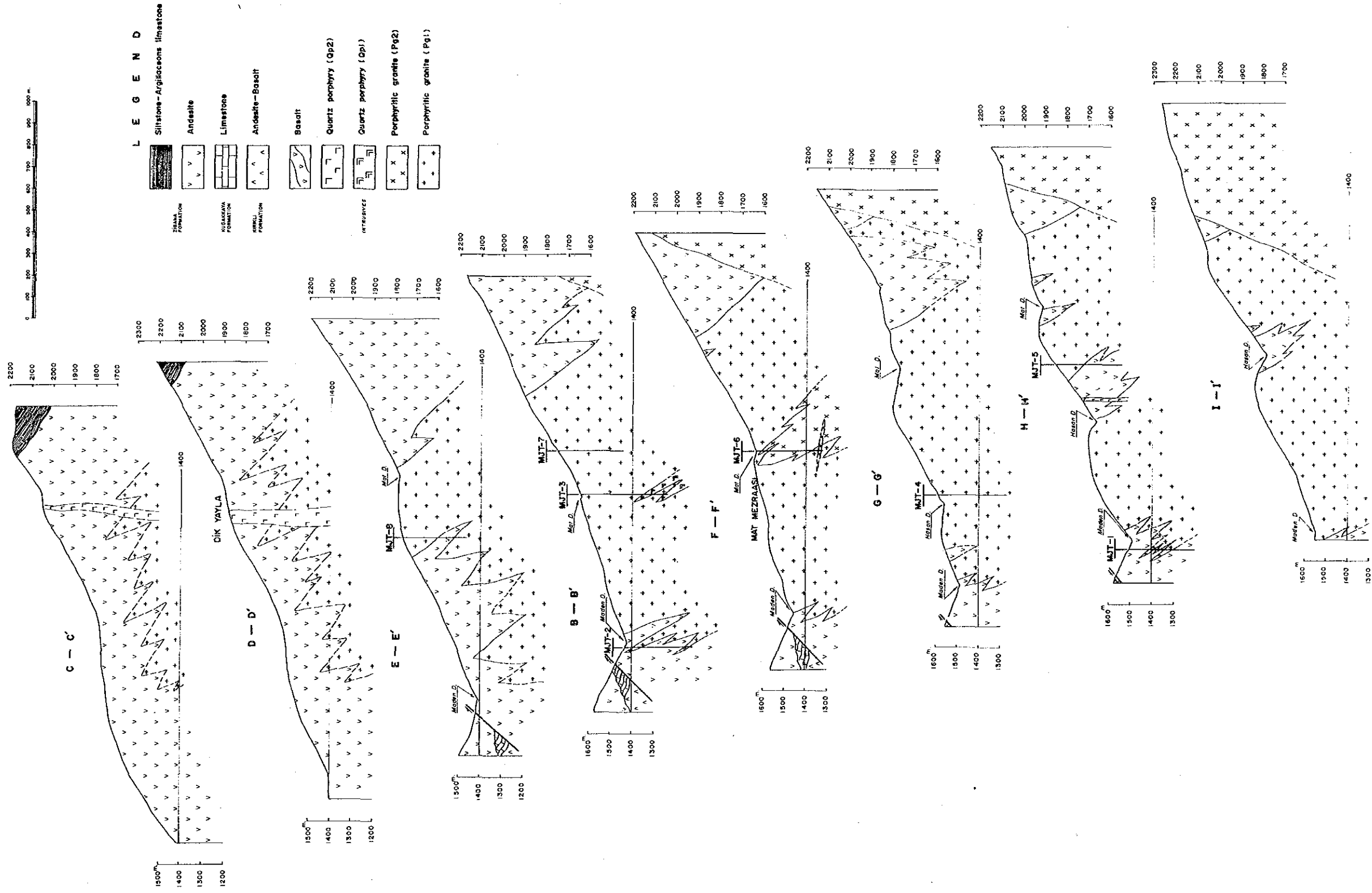


Fig. 52 Geological Profiles of Geophysical Line

GEOLOGICAL PROFILES OF GÜZELYAYLA MINERALIZED ZONE

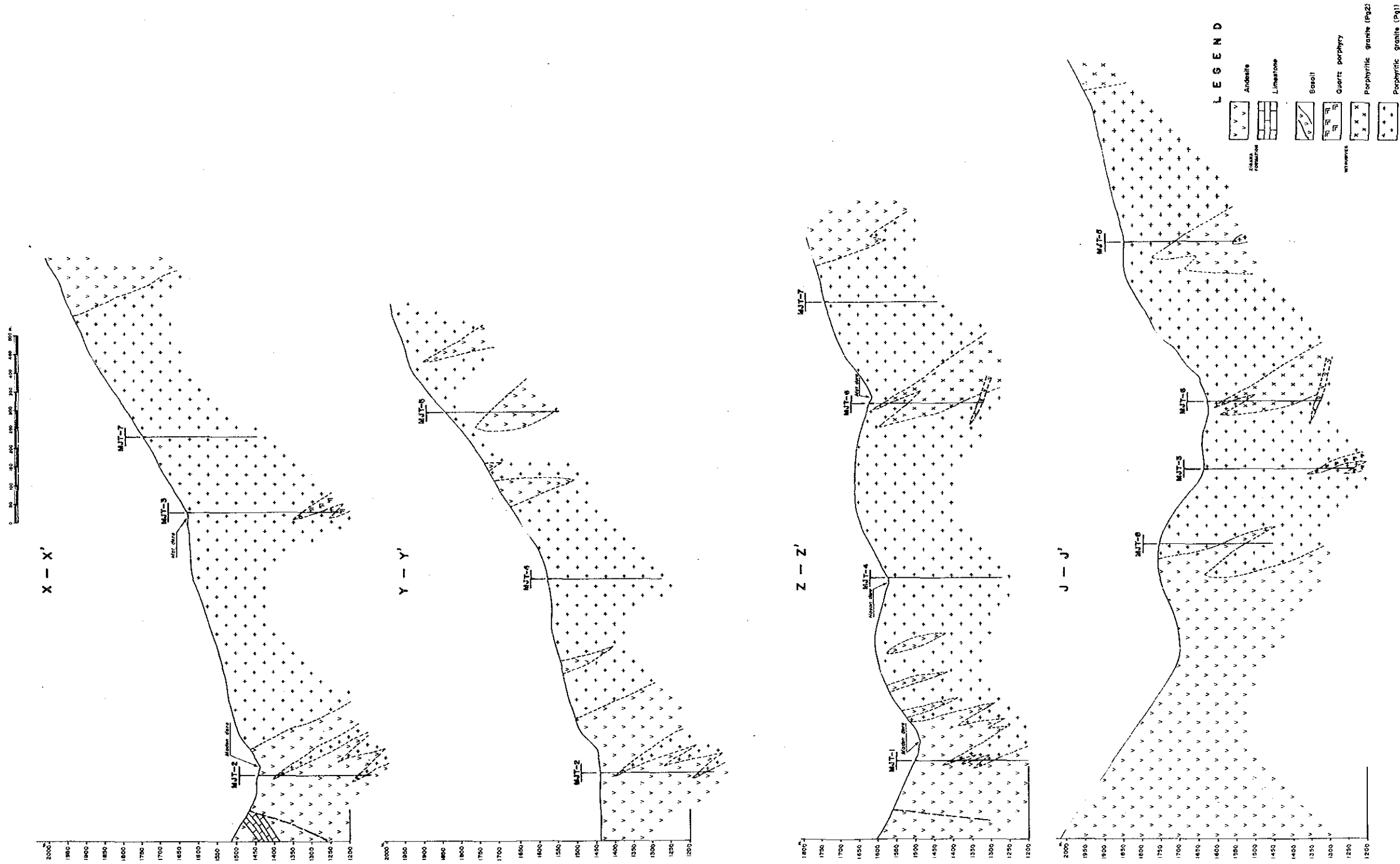


Fig. 53 Geological Profiles of Drill Holes

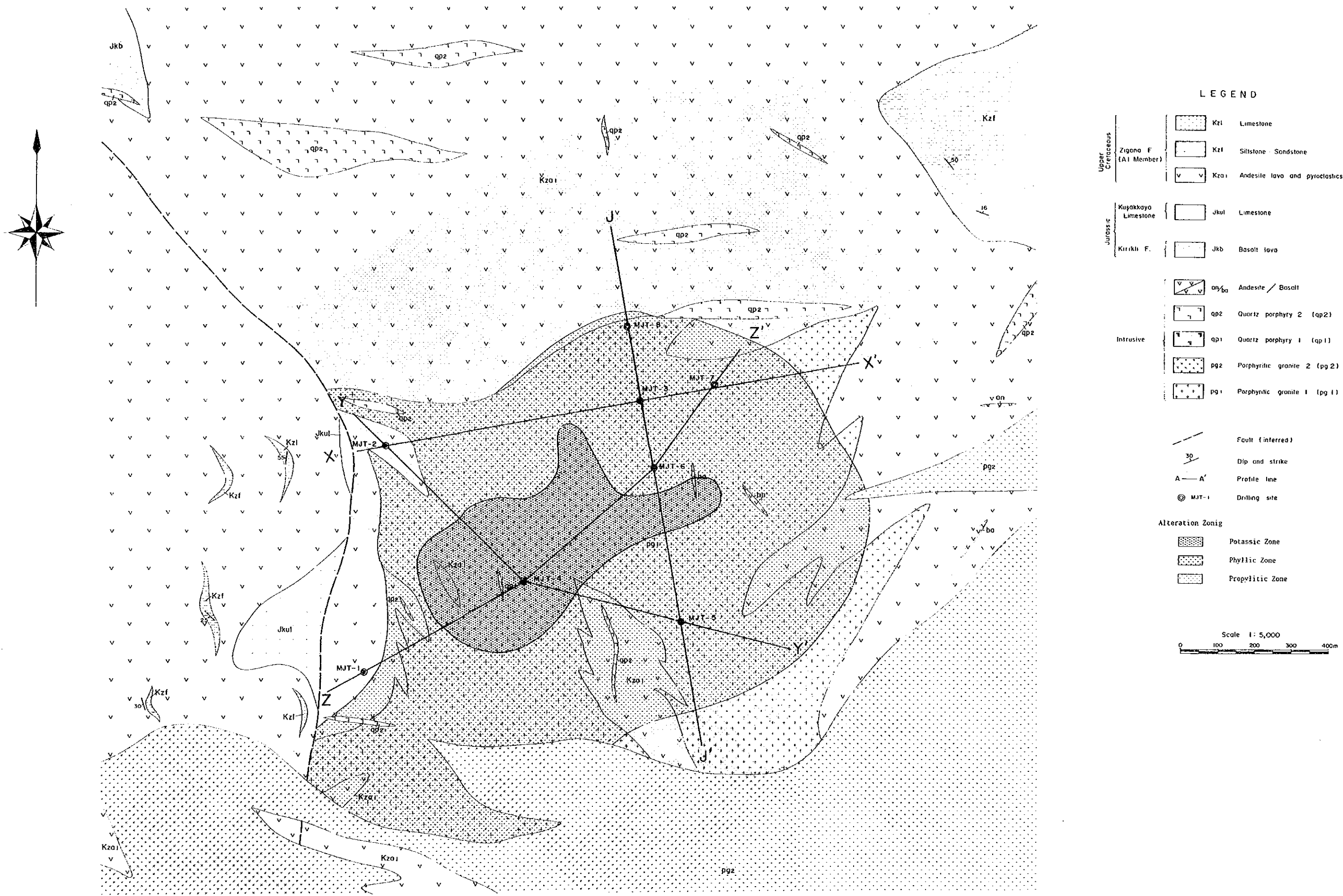


Fig. 54 Alteration Zoning Map of Drill Holes

GEOLOGICAL PROFILES OF GÜZELYAYLA MINERALIZED ZONE

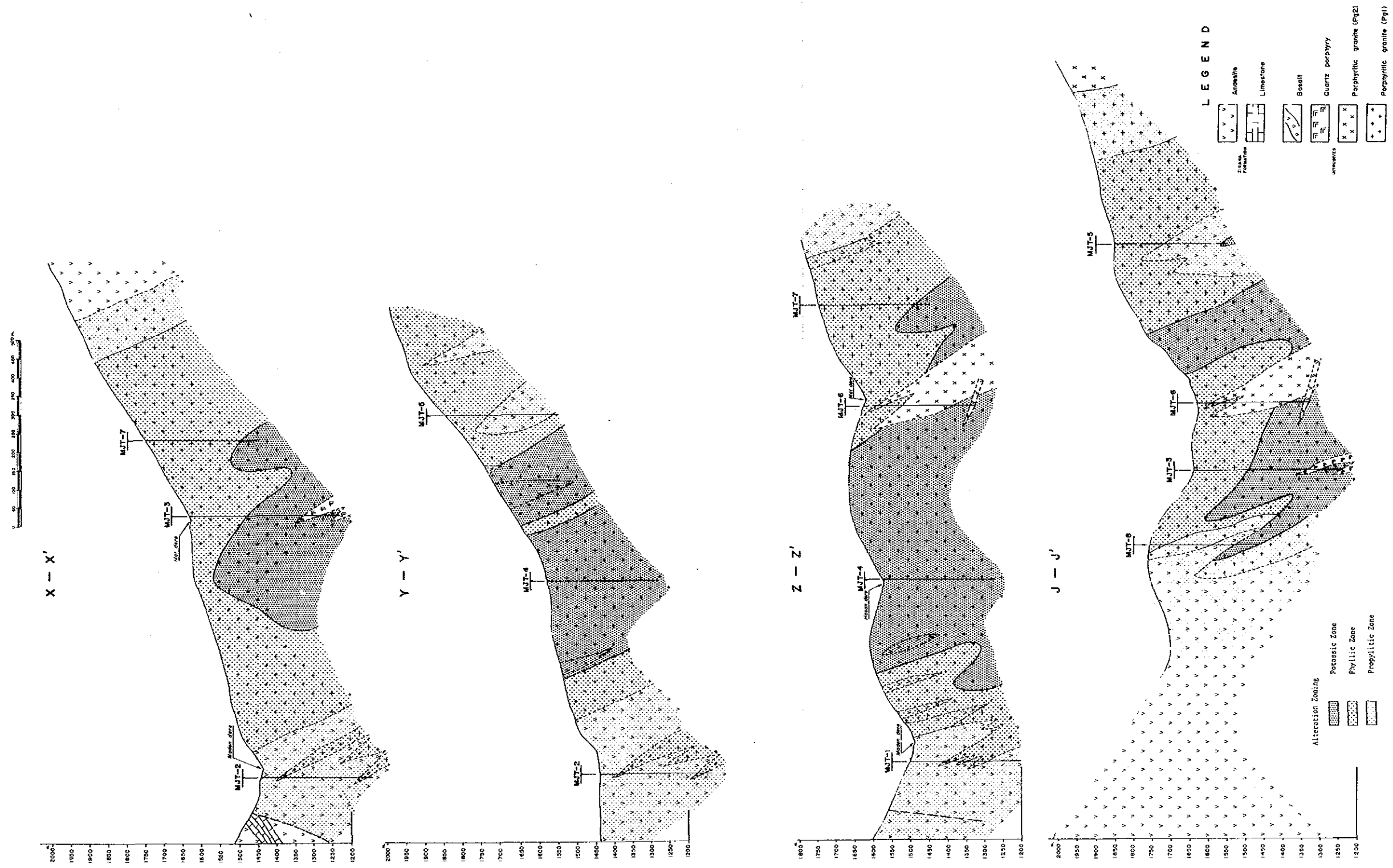


Fig. 55 Alteration Zoning Profiles of Drill Holes

Table 22 List of X-ray Diffraction Analysis (No 1)

Location	Sample No.	Minerals																	
		m	mix	ch	se	bi	k	q	kf	pl	ca	do	gy	anh	mo	py	mt	ho	
MJT-4	15.00m	☐			☐	○	○	⊙	☐							☐			
	30.00m			☐	☐	☐	☐	⊙	○	○						☐			
	45.00m			☐	☐	☐	☐	⊙	○	○						△			
	60.00m			☐	☐	☐	☐	⊙	○	⊙									
	75.00m			☐	☐	○	☐	○	○	⊙									
	90.00m	○		☐	☐	☐	○	⊙		○						☐			
	105.00m	☐		☐	☐	○		⊙		⊙						☐			
	120.00m			☐	☐	○		⊙		○						☐			
	135.00m			○	☐	☐		⊙		⊙						△			
	150.00m			☐	○	☐		⊙		⊙						△			
	165.00m			☐	☐	☐		⊙	○	⊙						☐			
	180.00m			☐	☐	○		⊙	○	○						☐			
	195.00m			☐	○	☐		⊙	○	⊙						△			
	210.00m			☐	☐			⊙	○	○						△			
	225.00m			☐	☐	☐		⊙	○	⊙						☐			
	240.00m			☐	☐	☐		⊙		⊙						△			
	255.00m			○	☐	☐		⊙	○	○						☐			
	270.00m			○	☐	○		⊙	○	○						☐			
	285.00m			○	☐	☐		⊙	☐	⊙					☐	△			
	300.00m			☐	☐	☐		⊙	⊙	⊙									
	MJT-5	15.00m			☐	○			⊙		☐						☐		
		30.00m			☐	○			⊙		⊙						☐		
		45.00m			☐	○			⊙		○						☐		
		60.00m			☐	○			⊙		○						☐		
		75.00m			☐	○			⊙		○						☐		
		90.00m			☐	○			⊙								☐		
		105.00m			△	○			⊙								☐		
		120.00m			☐	○			⊙								☐		
		135.00m			○	○			⊙		○	☐					☐		☐
		150.00m			☐	☐			⊙		○						☐		
165.00m				☐	☐			⊙		○	☐					☐			
180.00m				☐	☐			⊙		⊙						☐			
195.00m				☐	○			⊙		○	△					△		☐	
210.00m				○	○			⊙		⊙	☐					☐		○	
225.00m				○	○			⊙		○	☐					☐		☐	
240.00m			○	○			⊙		○						☐		☐		
255.00m			○	○			⊙		⊙						☐		☐		
270.00m			⊙	○			⊙		○						☐		☐		
285.00m			○	○			⊙		○	☐					☐		△		
300.00m			☐	○			⊙		○	☐					☐				
MJT-6	15.00m			☐	○			⊙		○	☐				☐				
	30.00m			☐	○			⊙		○	☐					△			
	45.00m			☐	○			⊙		○	☐					☐			
	60.00m			☐	○			⊙		☐	☐					☐			
	68.20m			☐	○			⊙				☐			△	△			
	75.00m			☐	○			⊙		○	☐				△	△			
	90.00m		☐	☐	○			⊙		○	☐				△	△			
	105.00m			☐	○			⊙		○	☐				△	△			
	120.00m			☐	☐			⊙		⊙	☐				△	△			
	135.00m			☐	☐			⊙		⊙	☐							☐	

Table 22 List of X-ray Diffraction Analysis (No 2)

Location	Sample No.	Minerals															
		m	mix	ch	se	bi	k	q	kf	pl	ca	do	gy	anh	mo	py	mt
MJT-6	150.00m			□	□			⊙		⊙	□						□
	165.00m			□	□			⊙	○	⊙	□					□	□
	180.00m			□	□			⊙	□	⊙	□				△	△	□
	195.00m			□	□		□	⊙		⊙	□					□	□
	210.00m			□	△			○	○	⊙	△					△	□
	225.00m			□	□			⊙	○	⊙	□					△	□
	240.00m			□	□			⊙		⊙	□					△	□
	270.00m			□	○			⊙		□	□		△	○	△	△	
	285.00m			□	○			⊙		□	□		△	○	△	△	
	301.00m			□	□			⊙		⊙	□			□			□
MJT-7	15.00m			□	□			⊙		⊙	□						□
	30.00m			□	○			⊙		○	□					△	
	45.00m			□	○			⊙		⊙	□					□	
	60.00m			□	○			⊙		⊙						△	
	75.00m			□	○			⊙	□	□						□	
	90.00m			□	⊙			⊙		□						△	
	105.00m			□	○			⊙							□	□	
	120.00m			□	○			⊙		○	□				□	△	
	135.00m			□	○			⊙		⊙					△	□	
	150.00m				○			⊙								△	
	165.00m			□	□			⊙		⊙	□				△	□	
	180.00m			□	○			⊙		○	□					△	
	195.00m			□	○			⊙		○	□				□	□	
	210.00m			□	○			⊙		○	△					△	
	225.00m				○		□	⊙		○	□	□			△	△	
240.00m			□	○		□	⊙		○	□					□		
255.00m			□	○			⊙		□			□		△	□		
270.00m			□	○			⊙		○	□		□			□		
285.00m			○	□			⊙		○	□			○		△		
300.00m			□	○			⊙		○	□			○		△		
MJT-8	15.00m			□	○			⊙		○						△	
	30.00m			□	○			⊙	□	□						□	
	45.00m			○	○			⊙		○					□	□	
	60.00m			⊙	○			⊙	□							□	
	75.00m			○	○			⊙	□							△	
	90.00m			○	○			⊙		○	△					□	□
	105.00m			⊙	○			○	□	○	□				□	□	□
	120.00m			○	□			○		⊙						△	□
	135.00m			○	○			⊙		○						△	
	150.00m			□	○			⊙								□	
	165.00m			○	○			⊙		□	△				△	△	
	180.00m			○	⊙			□								□	
	195.00m			○	○			⊙	□	□						□	
	210.00m			○	⊙			⊙	△	□	△					△	
	225.00m			⊙	○			⊙	□	○						□	
240.00m			○	○	□		⊙	□	○						□		
255.00m			□	○	□		⊙		⊙						□		
270.00m			○	○	□		⊙	□	○						□	□	
285.00m			□	○			⊙	□	○						□		
300.00m			□	○			⊙		○						△		

⊙ : >30 ○ : 10~29.9 □ : 1~9.9 △ : <0.9

and phase value. These values fall slightly east of the MJT-3 site.

- ② Among SIP responses obtained from laboratory tests of cores and rock samples, PFE and phase values are in proportional correlation, while both values and resistivity values have inversely proportional correlation. The relation between copper or molybdenum grades and SIP response is that there is no correlation. Phase spectra of the higher copper grade section is similar to spectra type of the non mineralized area (general type spectra).

The above mentioned SIP survey results indicate that the high PFE value (phase value) anomaly is caused by pyrite emplacement. Determination of a pyrite rich zone by geophysical survey and by consideration of geological and alteration conditions is very useful for finding copper rich zones which may surround the pyrite.

Results of IP and SIP methods (third phase)

A zone consisting of high PFE and high phase values was found on the periphery of the altered porphyritic granite (Pg1). The zone forms an arc of a circle because of the distribution area of the unaltered porphyritic granite. A north-south direction of another zone of high PFE and high phase was disclosed in the central portion within the arc of a circle.

The results of the geophysical surveys in the second and third phases indicate that the high PFE value (phase value) anomaly is caused by pyrite emplacement. Drilling sites in the third phase were determined on the basis of the geophysical data. MJT-7 and MJT-8 were drilled inside an arc of a circle. The Relations between drilling and geophysical survey results are as follows;

	Geophysical survey(PFE)	Results of drilling
MJT-4	0~ 300m > 8%	5~ 150m :Weak mineralization
	300m~ < 8%	150m~ :Mo-Cu mineralized zone
MJT-5	100~ 300m > 8%	10~ 100m :Secondary enrichment zone
	300m~ < 8%	100m~ :Pyrite-rich zone
MJT-6	100~ 250m > 8%	1~ 112m :Cu-Mo mineralized zone
		112~ 244m:unaltered porphyritic granite
		244m~ :Mo-Cu mineralized zone
MJT-7	0~ 300m < 8%	5~ 42m :Secondary enrichment zone
		42m~ :Weak mineralization
MJT-8	0~ 300m < 8%	9~ 84m :Secondary enrichment zone
		84~ 170m :Mo-Cu mineralization
		170m~ :Weak mineralization

Chapter 6 Fluid Inclusions

6-1 Measurement of Homogenization Temperature

Samples for measuring fluid inclusions were collected from drilling cores in the Güzelyayla area in which a promising porphyry copper ore deposit is expected. Samples were collected from the following rocks, and their amounts are as follows:

(1) Altered porphyritic granite (Pg1)	39 samples
(2) Unaltered porphyritic granite (Pg2)	8 samples
(3) Andesite (Zigana Formation)	3 samples
Total	50 samples

Among these samples, quartz veins and quartz phenocrysts were from the altered porphyritic granite (Pg1) (regarded as the ore-bringer intrusion) and the unaltered porphyritic granite (Pg2) (slightly post-intrusion of Pg1), and quartz veins bearing molybdenite in andesite intruded by Pg1 and Pg2 were collected for fluid inclusion measurements.

A Leitz microscope and heating stage of the type 1350 were used for heating laboratory work. Bichromate kalium (chemical reagent ; melting point : 394°C) was used for temperature correlation , and a galvanometer of 20°C scale was used for temperature reading (error: $\leq \pm 10^\circ\text{C}$). Fifty-nine specimens in total were prepared, but 9 specimens among them could not be measured as they were smaller than 10 μ in size.

After checking reproducibility of the temperature measurement, fluid inclusion measurements were carried out 5 or 6 times per specimen through this check. The error of reproducibility was almost $\pm 10^\circ\text{C}$. 1,004 fluid inclusions were measured from 50 samples collected. Measured fluid inclusions per sample ranged from 10 to 23 inclusions (average: 20 inclusions per sample). The number of measurements for each rock type and quartz samples are shown as follows:

	Phenocryst	Quartz vein	Total
Altered porphyritic granite (Pg1)	235 pcs	557 pcs	792 pcs
Unaltered porphyritic granite (Pg2)	70 pcs	82 pcs	152 pcs
Andesite (Zigana Formation)		60 pcs	60 pcs
Total	307 pcs	699 pcs	1,004 pcs

Homogenization temperatures measured are shown in Figs. 56~60 and in Tables 23 ~ 26.

As a result of the measurements, all homogenization temperatures range broadly between 320°C and 540°C, but 90% of these values are included within the range of 350°C to 450°C. Over 80% of the homogenization temperature values per sample are in the temperature range of 50°C to 100°C, showing normal distribution. Such a tendency is more predominant in the quartz vein than in the quartz phenocryst.

The measurable diameter of fluid inclusions is 20 μ to 30 μ , but sometimes, fluid inclusions 10 μ or several 10's of μ in diameter were also measured. Thin sections less than 0.3mm to 0.4mm in thickness with both planes polished, were prepared.

Many fluid inclusions were surrounded by transparent quartz. There were many inclusions less than 10 μ in diameter and ellipsoidal in form. Among these inclusions, negative quartz crystals were also observed, and pseudo secondary or secondary inclusions were of irregular form.

Fluid inclusions of core samples were characterised by a high ratio of the gaseous phase. Thus they were called gaseous phase inclusions.

Fluid inclusions of the Güzelyayla area contain polyphase inclusions, common in other porphyry copper deposits. They consist namely of gaseous inclusions which contain bubbles (over 60% of inclusion in volume) and little liquid and is wholly filled by gaseous inclusions owing to the expansion of gases after heating, and liquid inclusions, which contain ball-formed gaseous bubbles (10% ~ 40% of inclusion in volume) in liquid and is wholly filled by liquid after heating. The 1,004 fluid inclusions measured are divided into 835 (70%) of liquid and 169 (30%) of gaseous fluid inclusions. The homogenization temperature of the gaseous fluid inclusions is 20~30°C higher than that of liquid fluid inclusions, regardless of whether they are in rock, quartz vein or quartz phenocryst.

Most fluid inclusions in the quartz veins and quartz phenocrysts can be described as follows:

- ① Consisting of two phase inclusions (gaseous and liquid phases)
- ② Many liquid phase fluid inclusions usually contain carbon dioxide
- ③ A few solid phase inclusions are observable. Some solid phase inclusions disappear near 280°C, and others disappear at 580°C. The former may be NaCl crystallized tetrahedrally and the latter are somewhat round in shape but are of rather irregular form.
- ④ Minor amounts of polyphase inclusions are present.
- ⑤ Most fluid inclusions are generally tiny, namely smaller than 20 microns in size.

The mean values of the homogenization temperatures are 372~412°C in the quartz vein of Pg1, and 391~434°C in the quartz vein in andesite. It is 392°C for the total samples of both rocks. The mean value of those in quartz phenocrysts is 400°C, close to the value for the quartz vein of Pg1. It is made clear, as shown in Table 26, that even including the value from Pg2, the difference between the mean values is statistically insignificant.

Figs. 56 ~ 59 show the histograms of homogenization temperatures obtained from the respective drilling holes. In comparison with homogenization temperatures of fluid inclusions in quartz veins in each part of Pg1, the temperature is highest (413°C) at MJT-5 around Hasan Dere. That is, the temperature decreases towards the periphery of the Pg1 intrusion. The temperatures of the quartz veins in andesite have the same tendency-highest (440°C) at the molybdenum anomalous area of north Mat Dere.

Fluid inclusions in the quartz phenocrysts of Pg2 are characterized by their small size, while those of Pg1 are somewhat larger in size.

Solid-phase-like fluid inclusions are characteristically observed in samples of MJT-8 from Maden Dere. NaCl in MJT-8 disappeared at 280°C, and fluid inclusions in MJT-7 contained material like NaCl. Gaseous fluid inclusions are observable in core samples from MJT-4 to MJT-8. Samples from MJT-7 and MJT-8 contain many gaseous phase inclusions and their homogenization temperatures are usually high, as is consistent with the abovementioned pattern.

The mean homogenization temperature of all cores is 399°C, and this value is 13°C higher than the temperature in surface rocks. Comparing each rock facies, the homogenization temperature in core samples of andesite is slightly higher than that in surface andesite, but conversely, the temperature in core samples of Pg1 is lower than that in the surface rocks. That is to say, 406°C ~ 410°C in cores, in contrast with 430°C ~ 480°C in ground surface rocks at Mat and Hassan Deres.

The results indicate that the homogenization temperature of gaseous inclusions is generally higher than that of liquid phase inclusions. Although differences between the temperature of gaseous and liquid inclusions of each sulphide mineral type is not especially remarkable, it may be inferred that chalcopyrite was crystallized at the highest temperature conditions in the early stage, and molybdenite was successively formed at high temperature in the gaseous phase.

The homogenization temperatures in MJT-7 and MJT-8 gradually increase with increasing depth. Although some hole irregularities occur, holes from MJT-4 to MJT-6 also show an overall increase in temperature with depth.

6-2 Salinity in the Fluid Inclusions

The microscope NE (Nikon) for measurement under low temperature was used to measure salinity of fluid inclusions. The microscope is able to cool and heat the sample between -120°C and $+60^{\circ}\text{C}$ for freezing and defrosting of solid inclusions. Liquid nitrogen of -196°C was used for cooling, and thermister a thermometer (sensitivity : 0.3°C) was installed for reading temperatures.

The number of measureable samples were 27 pieces among 50 samples collected since most were small inclusions. It was very difficult to observe the phase variation at the melting point of frozen inclusions owing to poor liquid phase inclusions. The results of the measurements indicate that the melting range from the freezing point was from -5°C to -17°C , and the NaCl equivalent concentration values were calculated to be 4.8 wt% to 20.60 wt% using the H_2O -NaCl diagram.

All NaCl concentration values of inclusions and homogenization temperatures lie in the range from 7 wt% to 15 wt%, and from 310°C to 400°C in quartz veins, while those values in intrusive rocks, especially in Pgl, are more dispersed.

The relationship between the homogenization temperature and the salinity is shown in Fig. 60. The relationship indicates the following:

- ① The homogenization temperatures of most fluid inclusions are proportionally higher in salinities of higher concentration.
- ② The fluid inclusions in drilling core contains slightly higher salinity concentrations than those in quartz veins of andesite.
- ③ In the case of Pgl, the salinity is higher in the area of Hasan and Mat Deres, but is comparatively lower in the Maden Dere area. This corresponds with homogenization temperature.

In solid phase inclusions, hydrohalite usually occurs, but it is difficult to identify the hydrohalite in this area because the fluid inclusions are very small in size. In the case of simple crystal solid inclusions accompanied by NaCl and KCl crystals, salinity of the inclusions are detected by the volume of solid and liquid in the inclusions and calculation of the compositions of crystal salt and soluted salt (Takenouchi 1962).

Salinity values calculated by this method are shown as follows;

MJT-4 (quartz vein in Pgl, 37.7m)	35.3wt%
MJT-4 (quartz vein in Pgl, 253.0m)	46.1wt%
MJT-5 (quartz phenocryst in Pgl, 8.0m)	38.7wt%
MJT-7 (quartz vein in Pgl, 16.0m)	30.8wt%
MJT-7 (quartz phenocryst in Pgl, 105.0m)	37.8wt%

KCl may not be present because no solid inclusions disappeared at low

temperature. Salinity values are definitely different between the values in the core of the mineralized zone at Maden River and values from the marginal part in the mineralized zone around Maden River. The former are 35%~46% detected by salt volume in inclusions and the latter values range from 8% to 20% (freezing point ; -5°C to -17°C) as determined by the cooling stage method.

6-3 Conclusion of Measurement Results of Fluid Inclusions

Total results of fluid inclusions measured from drilling cores (MJT-4~MJT-8) are summarized in the following table.

Rock Name	Amount of Sample	Qz vein		Qz pheno		Qz vein+Qz pheno		Total	%
		Liquid	Gaseous	Liquid	Gaseous	Liquid	Gaseous		
Ande	2	48	12	-	-	48	12	60	6
Pg1	40	472	85	194	41	666	126	792	79
Pg2	8	56	26	65	5	121	31	152	15
Total	50	576	123	259	46	835	169	1,004	100
%		70		30		83	17	100	

(Qz:quartz, pheno:phenocryst, unit :piece)

The results of fluid inclusion measurements are summarized as follows;

- ① The homogenization temperature of fluid inclusions obtained from the quartz vein of the andesite in MJT-8 around Mat Dere is the highest. In the surface rock, gaseous inclusions in quartz veins and quartz phenocrysts are about 40°C ~ 50°C higher in temperature than those of liquid inclusions. In the core sample, gaseous inclusions are -1°C ~ 44°C (average 29°C) higher in temperature than those of liquid inclusions, showing a similar tendency as the samples from andesite. This fact presumes that this section in the center of the intrusive stock body of Pg1. The temperature falls slightly toward the deeper part. The fact that the homogenization temperature increases little by little toward the deeper part indicates that the Pg1 rock body inclines.
- ② The area where boiling phenomena might have taken place, owing to the presence of many gaseous inclusions, is located at and around the northern area of Mat dere. Fluid inclusions from drilling cores around the center are high in salinity because many solid inclusions are observable.
- ③ Fluid inclusions of Pg2 have slightly higher homogenization temperatures than those of Pg1. Also, gaseous inclusions in the former are smaller in scale than those of the latter.
- ④ A densely salinity ore solution was probably supplied to the area of Mat and Hasan Dere.

Table 23 List of Amount of Fluid Inclusion Samples

MJT-7

Depth(m)	V/P	Name and Description	Homoginiza.T		Salinity	
			Pcs	Average	Pcs	Average
14.45	P	Sericite Pgl	22	379	5	12.8
16.0	V	Sericite Pgl with qz(5mm)	20	371	*	*
56.0	V	Qz vein(10mm) in Pgl	22	367	7	11.0
74.0	V	Chl-ser Pgl with qz(4mm)	20	419	*	*
105.0	P	Ep-chl-ser Pgl with Mo	21	441	8	16.2
125.0	V	Qz vein(20mm) in Pgl	20	419	7	15.0
166.6	V	Qz vein(20mm) in Pgl	22	374	*	*
190.0	V	Silicified Pgl with qz(3mm)	20	375	7	13.3
244.8	V	Sericite Pgl with qz(2mm)	20	398	7	16.2
300.0	V	Silicified ser-anhydrite Pgl	20	435	9	15.4

MJT-8

Depth(m)	V/P	Name and Description	Homoginiza.T		Salinity	
			Pcs	Average	Pcs	Average
24.0	V	Mo-qz vein(8mm) in Pgl	22	386	6	13.8
46.6	V	Qz vein(5mm) in Pgl	18	383	*	*
66.1	V	Chl-ser Pgl with Cc and qz	22	396	6	14.9
131.0	V	Mo qz vein(30mm) in Pgl	20	404	*	*
135.0	V	Chl-ser Pgl with qz(3mm)	20	411	*	*
146.95	V	Chl-ser Pgl with qz(6mm)	21	402	7	12.6
184.0	V	Mo qz vein(5mm) in andesite	20	440	3	15.4
225.0	V	Ser-chl Pgl with Mo qz(4mm)	20	422	*	*
274.7	V	Magnetite-Py qz(25mm) in Pgl	20	466	*	*
298.5	V	Mo qz vein(10mm) in Pgl	20	410	7	15.0

Abbreviations

- Rock name Pgl: Altered porphyritic granite
 Pg2: Unaltered porphyritic granite
 Minerals Qz: Quartz Cp: Chalcopyrite
 Ch: Chlorite Py: Pyrite
 Ser: Sericite Mo: Molybdenite
 Bio: Biotite Cc: Chalcocite
 Mag: Magnetite Cv: Covellite
 V/P V: Quartz vein P: Quartz phenocryst
 Homoginiza.T Homoginization Temperature (°C)
 Salinity NaCl wt %
 * ; Impossible to Measure Salinity of Fluid Inclusion

MJT-4

Depth(m)	V/P	Name and Description	Homoginiza.T		Salinity	
			Pcs	Average	Pcs	Average
19.0	V	Sericite Pgl with qz(5mm)	20	364	8	13.2
37.7	V	Bio-ser Pgl with qz(5mm)	22	395	9	14.6
60.0	P	Biotite Pgl	20	372	*	*
72.1	P	Chl-bio Pgl	22	367	7	11.7
81.6	V	Chl-bio Pgl with qz(6mm)	22	355	*	*
109.0	P	Bio(chl) Pgl	22	424	*	*
116.8	V	Bio Pgl with qz(8mm)	22	382	6	12.3
180.4	V	Chl-bio Pgl with qz(7mm)	22	379	8	13.8
253.0	V	Chl-bio-ser Pgl with qz(5mm)	22	373	9	14.6
280.7	V	Chl-bio-Pgl with qz(1~2mm)	22	419	*	*

MJT-5

Depth(m)	V/P	Name and Description	Homoginiza.T		Salinity	
			Pcs	Average	Pcs	Average
5.0	P	Sericite Pgl	22	433	*	*
8.0	P	Sericite Pgl	20	448	6	17.3
36.4	P	Sericite Pgl	22	416	*	*
49.0	P	Sericite Pgl with Cc & Cp	20	423	6	14.5
65.3	V	Sericite Pgl with Cc & Cp	20	421	7	13.3
75.5	V	Mo qz (4mm) in Pgl	20	406	*	*
99.0	P	Sericite Pgl	20	392	*	*
133.4	P	Sericite Pgl	11	386	*	*
141.7	V	Py qz vein (10mm) in andesite	20	380	6	13.5
261.4	V	Mo qz vein (10mm) in andesite	20	409	8	16.8

MJT-6

Depth(m)	V/P	Name and Description	Homoginiza.T		Salinity	
			Pcs	Average	Pcs	Average
40.0	P	Chl-sericite Pgl	13	382	*	*
73.0	V	Silicified chl-sericite Pgl	20	398	6	10.4
85.3	V	Silicified chl-sericite Pgl	18	385	5	10.9
112.6	P	Intrusive rock (Pg2)	17	406	*	*
123.0	V	Segregated qz in Pg2	20	402	7	13.5
123.0	P	Intrusive rock (Pg2)	20	396	*	*
124.5	V	Segregated qz in Pg2	22	397	8	14.7
128.0	P	Intrusive rock in Pg2	10	414	*	*
136.0	V	Segregated qz in Pg2	20	414	*	*
168.4	P	Intrusive rock (Pg2)	23	401	*	*

Table 24 List of Fluid Inclusion Samples on Sampling Items

V/P	Rock Name	Locality of sample	No of Sample	Sample Name
	Andesite (Zigana F)	MJT-5	2	141.7m, 261.4m
		MJT-8	1	184.0m
	Porphyritic granite (Pg1)	MJT-4	7	19.0m, 37.7m, 81.6m*, 116.8m, 180.4m, 253.0m*, 280.7m
		MJT-5	2	65.3m, 75.5m*
		MJT-6	1	85.3m
		MJT-7	8	16.0m, 56.0m, 74.0m, 125.0m, 166.6m*, 190.0m, 244.8m, 300m
		MJT-8	9	24.0m, 46.6*m, 66.1m, 131.0m*, 135.0*m, 146.35m, 225.0m, 274.7m, 298.5m
	Porphyritic granite(Pg2)	MJT-6	4	73.0m, 113.0m, 124.5m, 136.0m
	V		34	
	Porphyritic granite (Pg1)	MJT-4	3	60.0m, 72.1m, 109.0m
		MJT-5	6	5.0m*, 8.0m, 36.4m, 49.0m, 99.0m*, 133.4m*
		MJT-6	1	40.0m
		MJT-7	2	14.45m, 105.0m
		MJT-8	-	
	Porphyritic granite(Pg2)	MJT-6	4	112.6m*, 123.0m, 128.0m, 168.4m*
	P		16	
	V+P		50	

*:Abundance of micro-fluid inclusion

Table 25 List of Homogenization Temperatures(Gaseous/Liquid Fluid Inclusions)

V/P	Rock Name	Locality of sample	Liquid Inclusion		Gaseous Inclusion	
			No of M.I	Homogenization T.	No of M.I	Homogenization T.
	Andesite (Zigana F)	MJT-5	35	391	5	422
		MJT-8	13	434	7	450
	Porphyritic granite (Pg1)	MJT-4	130	372	22	416
		MJT-5	38	412	2	435
		MJT-6	13	385	5	384
		MJT-7	147	391	17	424
	MJT-8	144	401	39	437	
	Porphyritic granite(Pg2)	MJT-6	56	399	26	409
V			576	392	123	423
	Porphyritic granite (Pg1)	MJT-4	52	381	12	415
		MJT-5	92	413	23	444
		MJT-6	8	373	5	396
		MJT-7	42	395	1	400
	MJT-8	-	-	-	-	
	Porphyritic granite(Pg2)	MJT-6	65	403	5	400
P			259	400	46	423
V+P		835	394	169	423	

Table 26 List of Homogenization Temperatures of Fluid Inclusions

V/P	Rock Name	Locality of sample	No of Sample	No of Inclusions	Range of Temperature(°C)	Mean value(°C)
	Andesite	MJT-5	2	40	340~450	395
	(Zigana F)	MJT-8	1	20	380~490	440
	Porphyritic granite (Pg1)	MJT-4	7	152	320~460	378
		MJT-5	2	40	350~480	413
	Porphyritic granite (Pg2)	MJT-6	1	18	360~420	385
		MJT-7	8	164	330~480	397
	V	MJT-8	9	183	380~540	409
		MJT-6	4	82	380~470	402
	Porphyritic granite (Pg1)		34	699		397
		MJT-4	3	64	330~450	394
		MJT-5	6	115	340~490	418
		MJT-6	1	13	340~410	382
		MJT-7	2	43	320~460	409
	Porphyritic granite (Pg2)	MJT-8	-	-		
		MJT-6	4	70	320~450	403
	P		16	307		403
	V+P		50	1,004		399

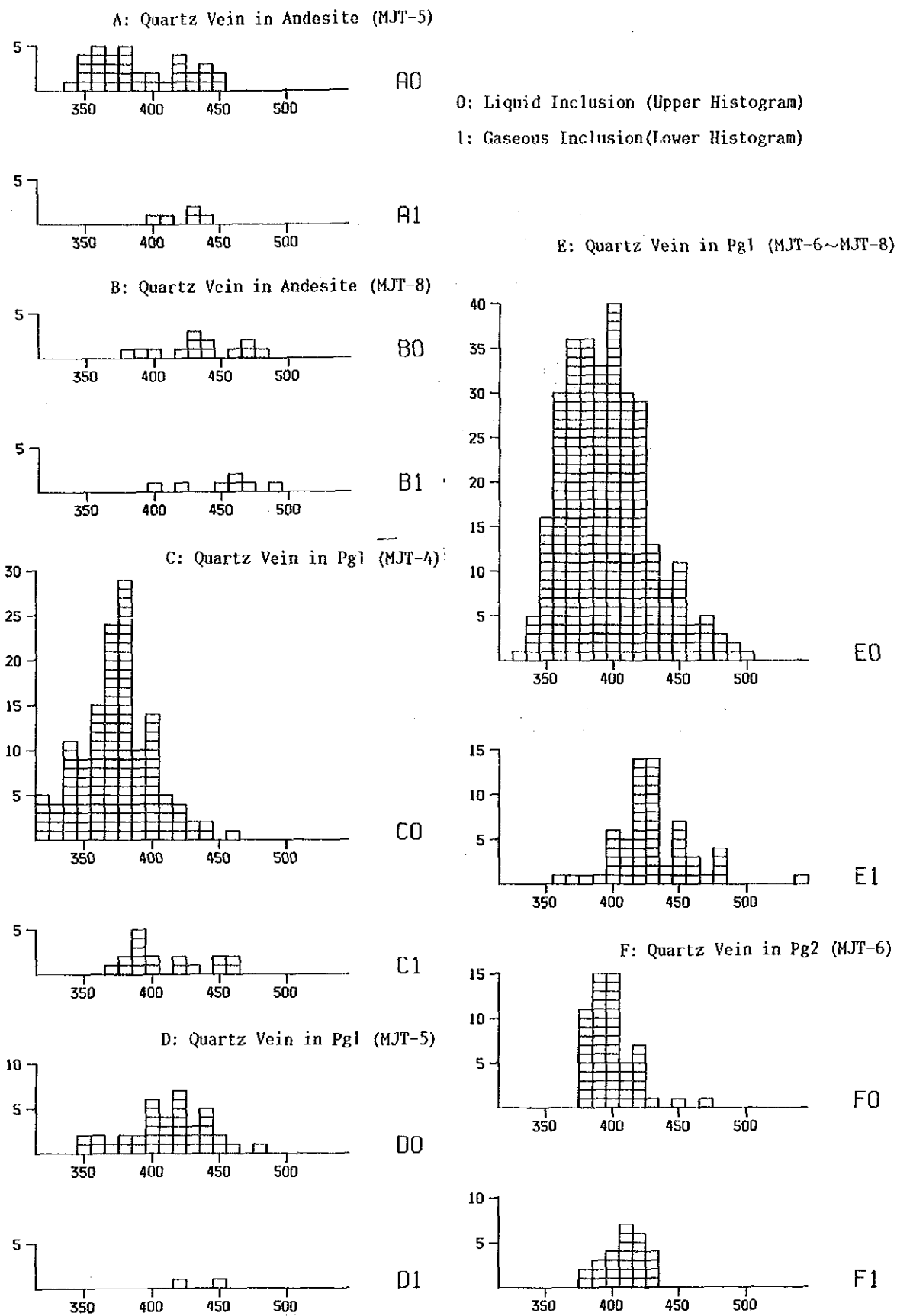
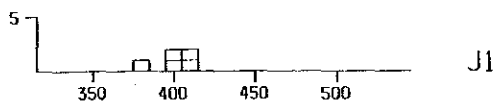
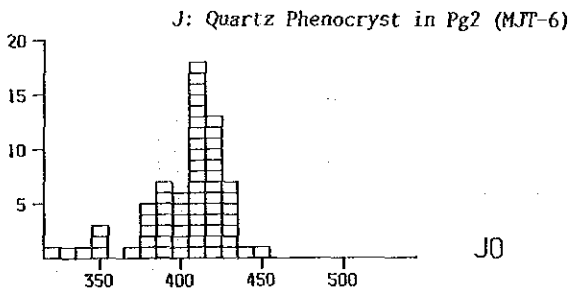
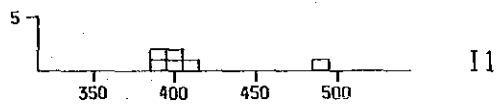
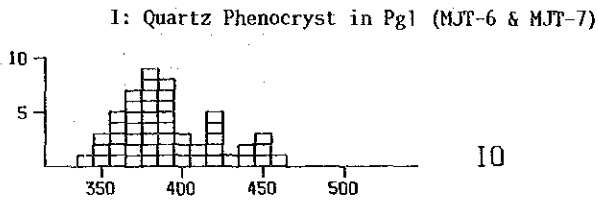
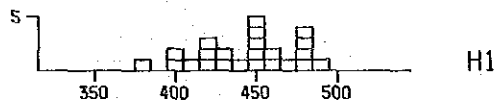
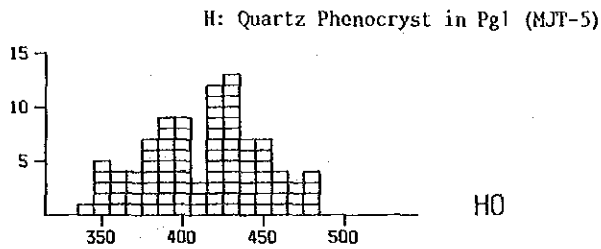
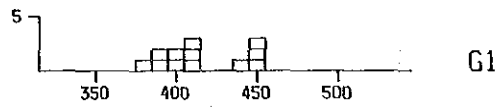
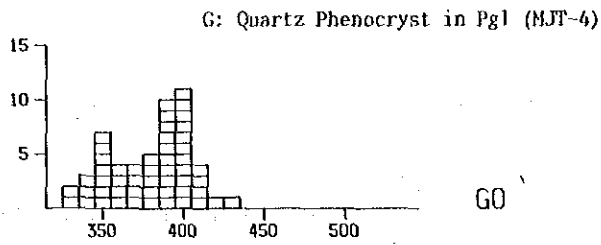


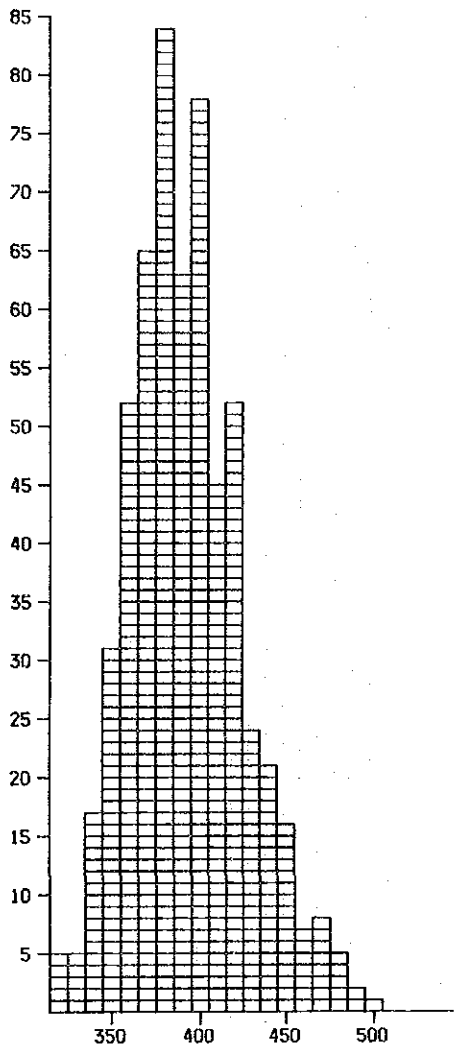
Fig. 56 Histogram of Homogenization Temperature (No 1)



0: Liquid Inclusion (Upper Histogram)

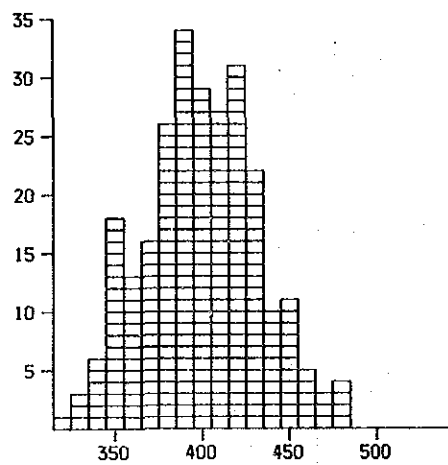
1: Gaseous Inclusion (Lower Histogram)

Fig. 56 Histogram of Homogenization Temperature (No 2)

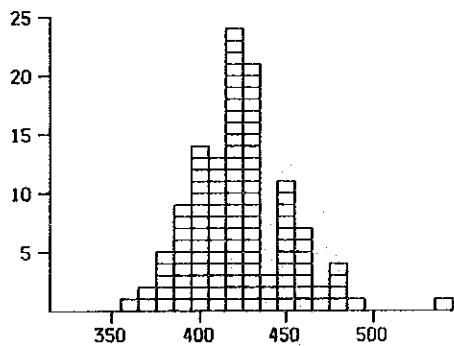


0: Liquid Inclusion (Upper Histogram)
 1: Gaseous Inclusion (Lower Histogram)

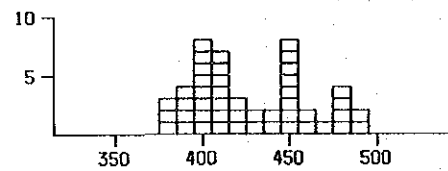
V0



P0



V1



P1

Fig. 58 Histogram of Homogenization Temperature (Quartz Phenocryst)

Fig. 57 Histogram of Homogenization Temperature (Quartz Vein)

0: Liquid Inclusion (Upper Histogram)
 1: Gaseous Inclusion (Lower Histogram)

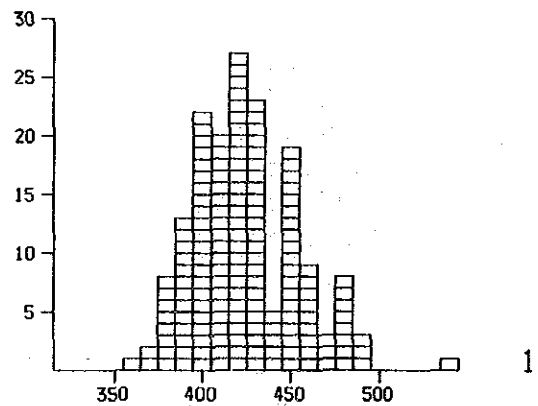
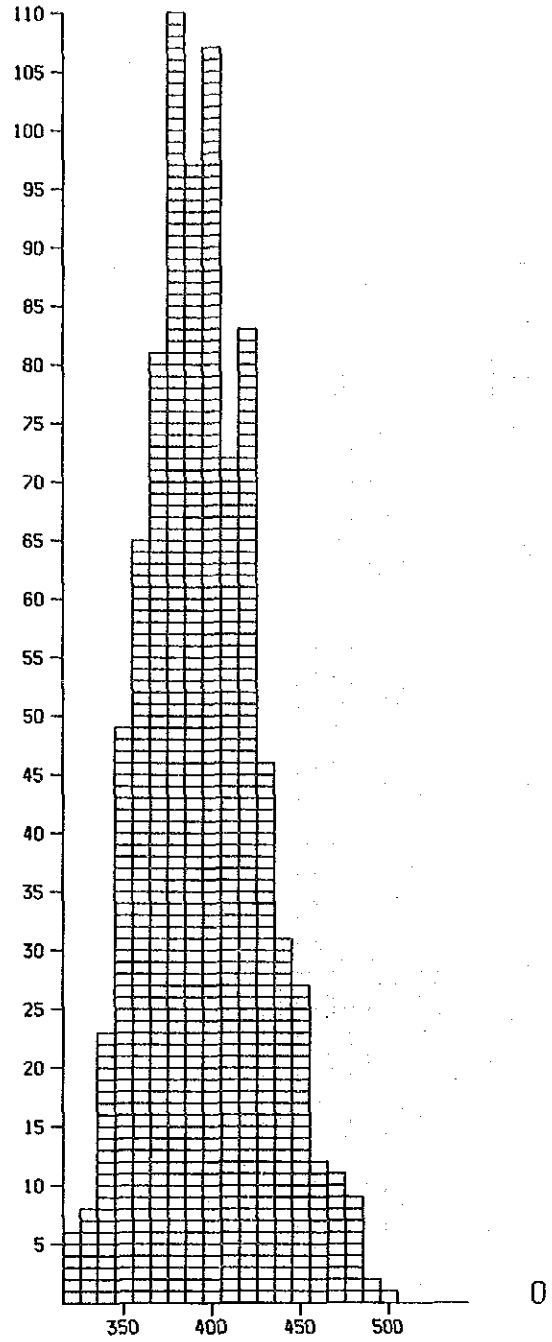
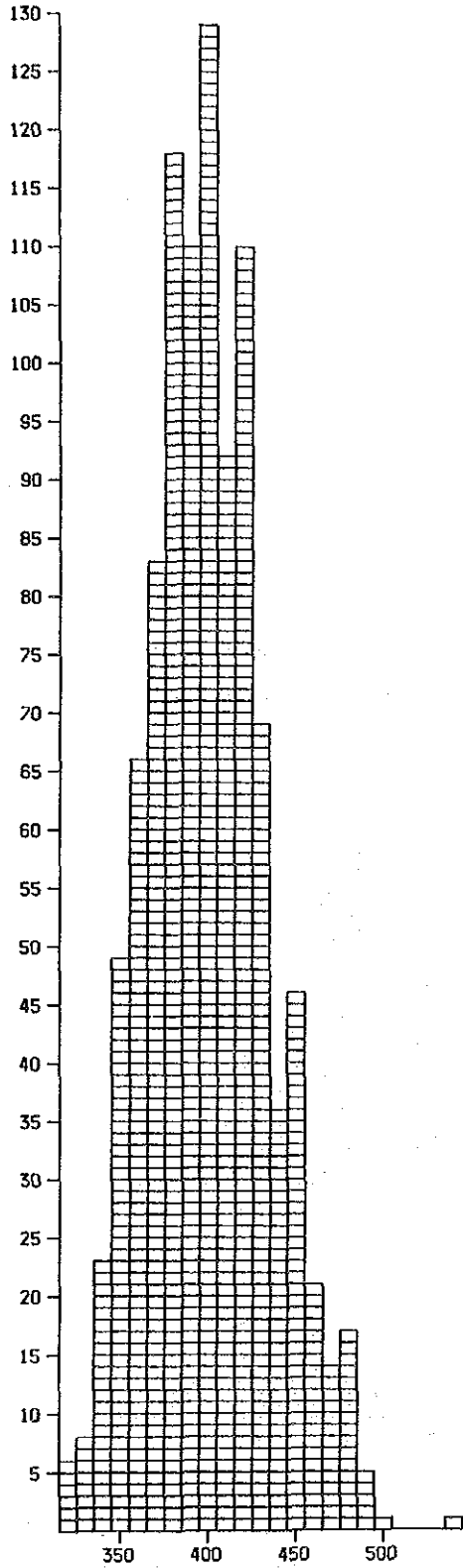
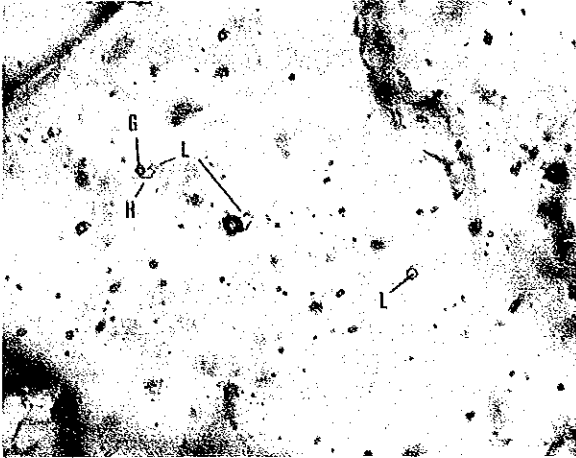
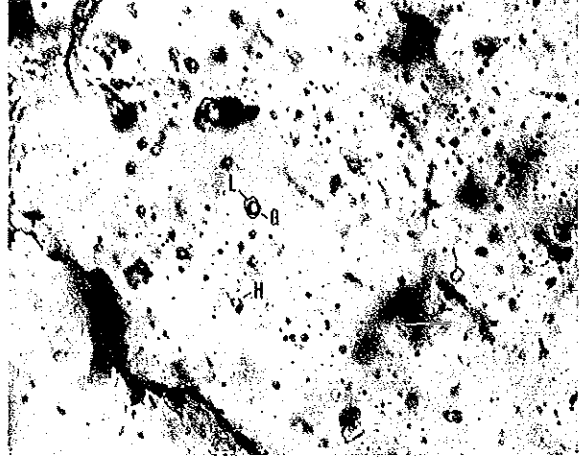


Fig. 59 Histogram of Homogenization Temperature (Gas/Liq Phase)

MJT-4 37.7m



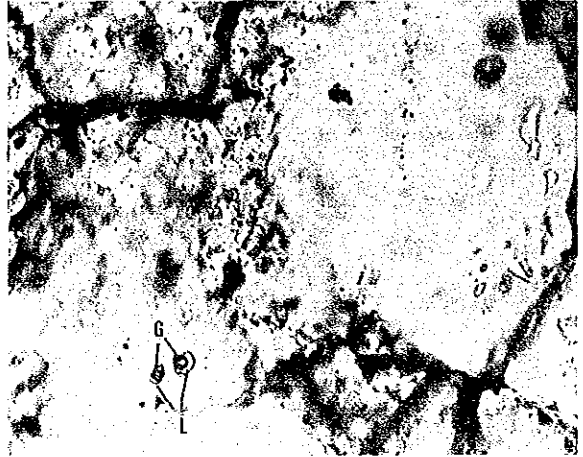
MJT-4 253.0m



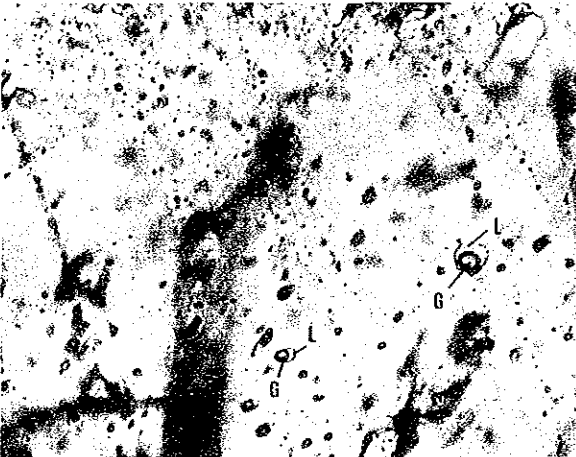
MJT-5 8.0m



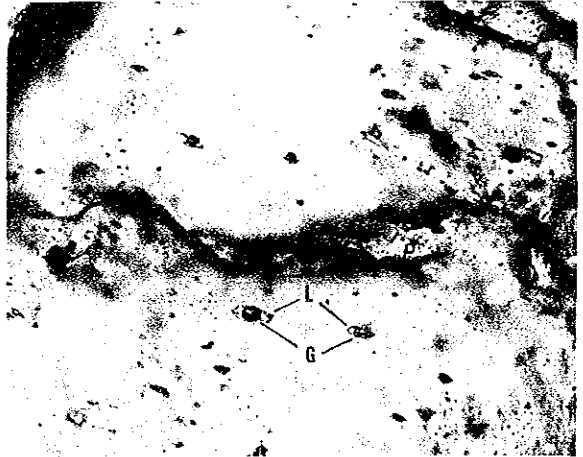
MJT-5 141.7m



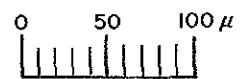
MJT-5 261.4m



MJT-6 73.0m

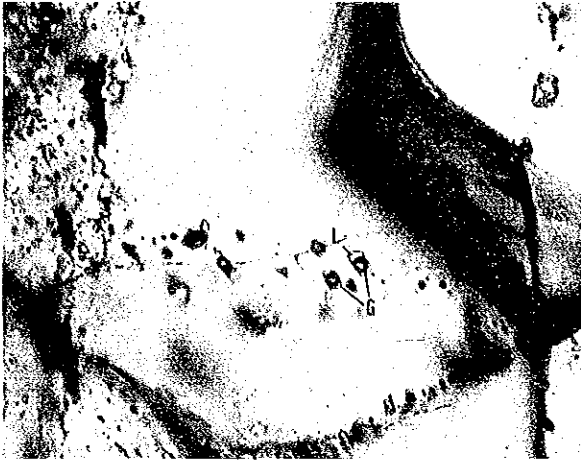


L : Liquid G : Gaseous H : Halite



Photograph Microscopic Photographs of Fluid Inclusions (No 1)

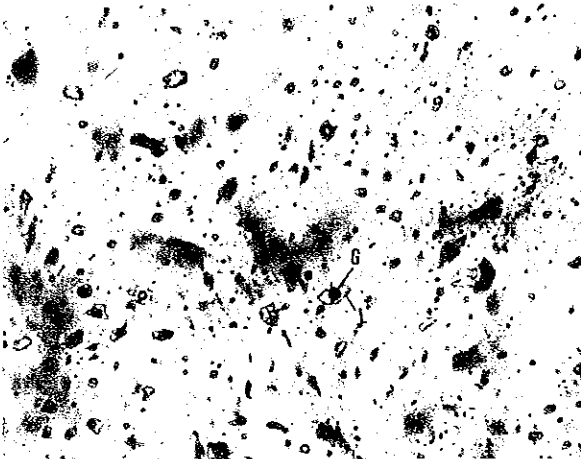
MJT-6 124.5m



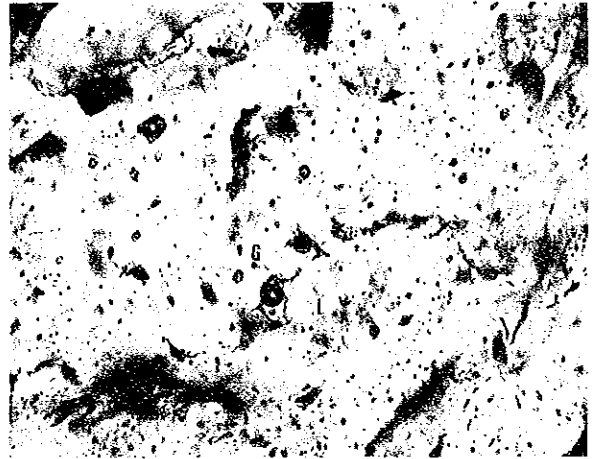
MJT-7 16.0m



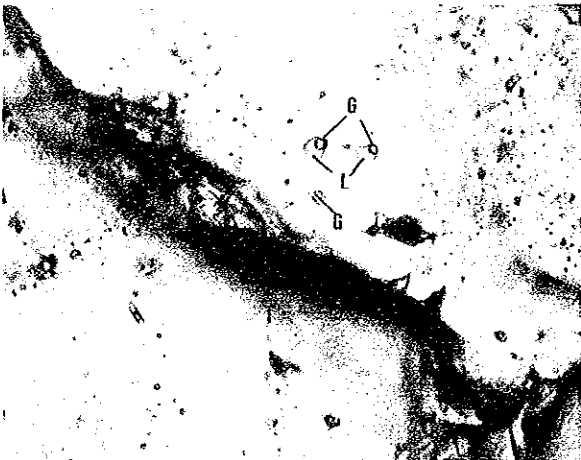
MJT-7 74.0m



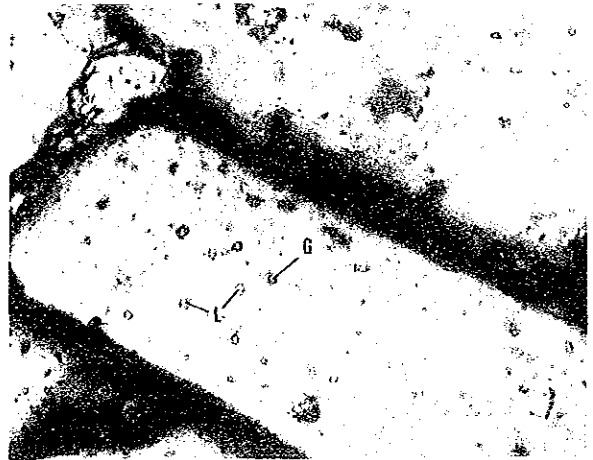
MJT-7 190.0m



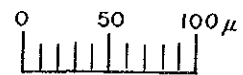
MJT-8 24.0m



MJT-8 184.0m



L : Liquid G : Gaseous H : Halite



Photograph Microscopic Photographs of Fluid Inclusions (No 2)

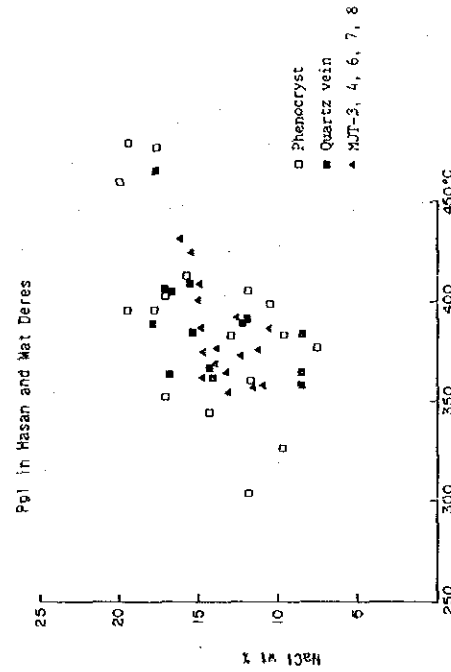
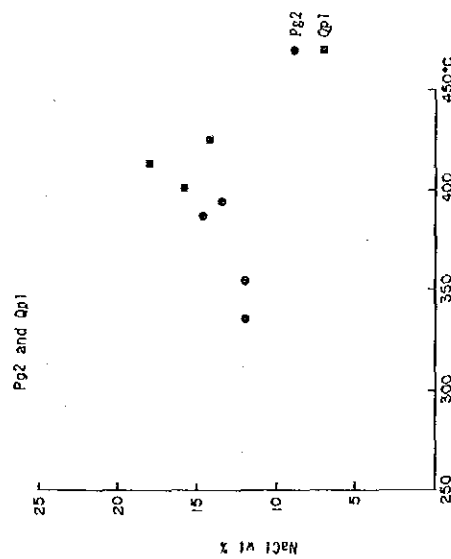
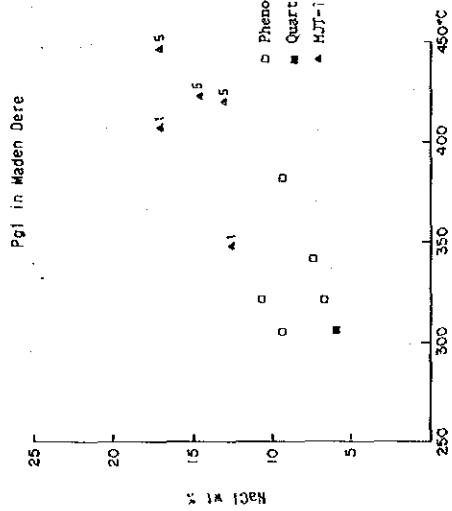
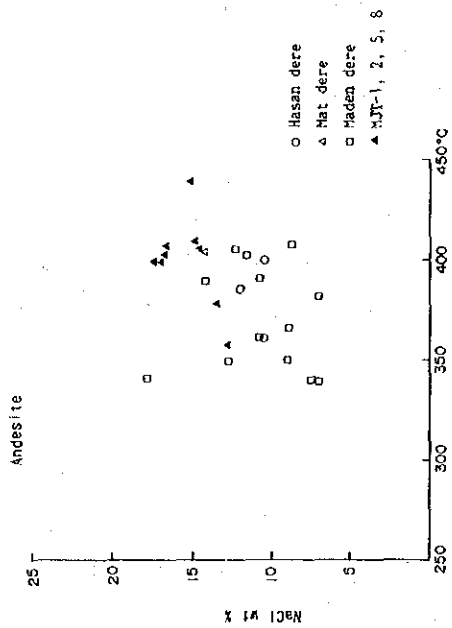


Fig 60 Relationship between Homogenization Temperature and Salinity

Chapter 7 Conclusions and Recommendations

Many ore deposits and mineral showings are known in the survey area. A small amount of mines were operated in the past, but most of them have not been explored. These ore deposits and mineral showings are classified into skarn, vein, and dissemination types.

Dissemination type ore deposits in particular, were not noticeable until recently because of low grade ore content. In fact, disseminated mineral showings have only recently been reported. In the area, the stock body, which intruded during the period from the late Cretaceous to Eocene, was accompanied by such mineralization. The mineralization is structurally controlled by the shape of the stock and also by conditions in the marginal part of the stock. High grade ores tend to be emplaced in areas where fractures and faults are well-formed.

Two types of disseminated ore deposits are expected in the Gümüşhane Area. One is a copper-molybdenum bearing ore deposit and the other is a deposit containing copper, zinc and lead without molybdenum. The former ore deposit is distributed in the Güzelyayla Area and the latter ore deposit is present with skarn in the Karadağ Area.

7-1 Conclusions

Led by the discovery of a copper and molybdenum anomaly through the geochemical survey (stream sediment) conducted by the United Nations Development Program during the period from 1970 to 1974 in the Güzelyayla Area, geological and geochemical surveys (stream sediment) of the cooperative exploration survey were commenced in 1984. MTA also carried out an additional soil geochemical survey. The soil geochemical survey resulted in the detection of values of Cu and Mo five to nine times higher than values in stream sediments. The anomalous area of Cu and Mo was defined as having a range of 1.8 km X 1.8 km.

Alteration, as detected by X-ray diffraction analysis and microscopic observation, is zoned from the center of the altered porphyritic granite (Pgl) towards the margin as potassic zone → phyllic zone → propylitic zone. The core of Pgl is a potassic zone of alteration and the alteration changes to a phyllic zone in the periphery of Pgl. In andesite intruded by the Pgl stock, propylitic zones are commonly distributed, while the phyllic zone is present close to Pgl. The potassic zone is characterized by the presence of a small amount of potassic feldspar, biotite and many anhydrites, the phyllic zone mostly by 2M₁ type sericite, and the propylitic zone by chlorite and many

magnetites. The alteration pattern of this survey area resembles the pattern of the Ulutaş porphyry copper type ore deposit. A neighbour of this survey area, it lacks potassic feldspar, and biotitization of hornblende exists in mineralized granodioritic porphyry (Taylor and Fryer, 1980).

As a result of the discovery of a Cu and Mo mineralized zone through analysis of the Cu and Mo anomalies and of the three drill holes of the 2nd phase, five drill holes (1,505m) were conducted in the 3rd phase. Although grade of Cu and Mo varies, grade of Cu and Mo was, in general, low. However, it is remarkable that each drill hole intersected the secondary enrichment zone.

Fracture pattern is an important guide to exploring the mineralized zone, for example, in the planning of drilling inclination. Geological and core logging surveys were performed marking the regularity of fracture patterns in the intrusive rock (Pg1) and in the andesite intruded by Pg1. However, the survey could not define any regularity of fracture patterns in the rocks.

Mineralization paragenesis are mostly pyrite-quartz, pyrite-molybdenite-quartz, chalcopyrite-pyrite, and chalcopyrite-pyrite-quartz, all embedded along fissures. Mineralization in MJT-4 to MJT-8 are emplaced along fissures, with quartz veins and as disseminations in the rocks.

Fluid inclusions are mostly of gaseous and liquid phases smaller than 10 μ in size. Polyphase inclusions are included in very small amounts considering that it is a porphyry type ore deposit. Solid materials in the inclusions are mostly halite. Intruded rock contains a very small amount of gaseous inclusions. On the other hand, the potassic zone of altered porphyritic granite, distributed around the area from Mat Dere to Hasan Dere, contains a large quantity of gaseous inclusions. Their homogenization temperatures are higher compared with inclusions of other areas. Around this area, solid inclusions predominantly occur, and the co-existence of dense fluid inclusions (polyphase) and thin fluid inclusions (gaseous phase) reveals that those might have been boiling conditions at the formation time of these inclusions.

Results of the geophysical survey (IP and SIP methods) revealed that there are strong mineralizations accompanied by sulphide minerals in the periphery of the altered porphyritic granite (Pg1). A PFE anomaly is not obtained in the distribution area of the unaltered porphyritic granite (Pg2).

7-2 Recommendations for Future Exploration

As a result of the geological, geochemical, geophysical and drilling surveys carried out in the second and third phases, it is recommended that the following works be conducted in the most promising areas mentioned above.

- ① Drilling survey in the geophysically anomalous areas

- ② Secondary enriched zone survey in the upstream area of Hasan and Mat deres
- ③ Geophysical survey of the north area of the anomaly after a drilling survey has been conducted in the anomalous areas

It is recommended for further explorations that the above-mentioned drilling survey be carried out to confirm an ore deposit in the expected mineralized area. Drilling sites and the area for geophysical survey should be changed according to the results of preceding drill holes.

RECOMMENDATION MAP FOR GÜZELYAYLA AREA

0 50 100 150 200 250 300 350 400 450 500 m.

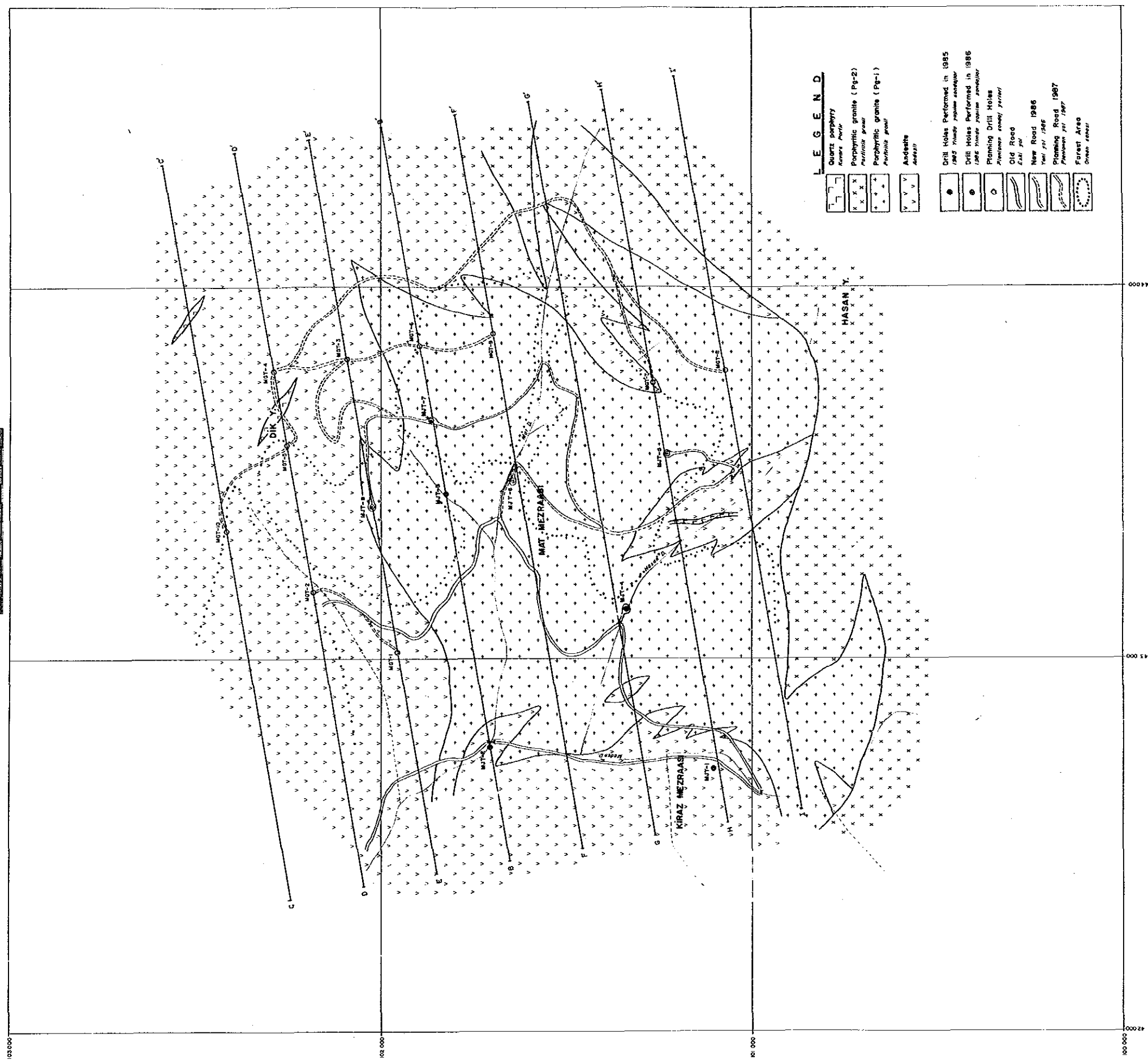


Fig. 61 Recommendation Map of Güzelyayla Area

Part 3 KARADAĞ AREA

Part 3 KARADAĞ AREA

Chapter 1 Outline of the Survey

1-1 Summary of the Initial and Second Phase Surveys

This survey area is situated in the Pontid Belt, and is characterized by plutonic intrusion activity in the period from the Late Cretaceous to the Eocene of the Tertiary. The surveyed area is located 8 km west of Altıntaşlar and is up stream of the Galis Dere. The old Karadağ mine is at around 2,500m above sea level. The geology around the old mine consists of Gümüşhane granite constituting the basement in the area and Upper Cretaceous andesite and Limestone (A1 Member) of the Zigana Formation. Quartz porphyry and granodiorite have intruded into the above mentioned basement and formations. Andesite and limestone of the Zigana Formation have undergone skarnitization, and an ore deposit may be embedded in the skarn. Primary sulphide ores, such as chalcopyrite and sphalerite, were found at the old mine site, but most ore minerals in outcrops have been oxidized, accompanied by secondary oxide copper. Cerusite was detected by X-ray diffraction analysis. Such an oxide ore zone is distributed along the limestone bed extending north-south over 1 km.

Chemical assay of chip samples revealed that the many ore samples contained considerable zinc and copper in the order of 10%. Such an oxidized copper zone can be traced over one km along the N-S striking limestone. This limestone stratum is displaced by a fault in the central part of the survey area. The copper-lead-zinc mineralized zone is distributed on the north side of the fault while the copper zone is on the south side of the fault, as indicated by the results of the chemical assay. Garnet and epidote are the main skarn minerals in the mineral showing, but the amounts of specularite and magnetite are very small compared to similar ore deposits including the Belen Tepe ore deposit at a nearby locality.

Disseminated mineral showings of the Karadağ Area containing copper or copper-zinc are embedded in the skarn and the stocks. Upon consideration of its geology and the condition of the ore deposit, it seems that the Karadağ ore deposit is a large scale deposit of copper (and iron). It is inferred that the mine is of similar type to the disseminated ore associated with tactite in the U.S.A. since rocks that have been intruded are limestone and andesite. This is the same condition as in the U.S.A. The Karadağ Mine might have been worked underground in very ancient times, and it seems that the high grade

section was selectively mined. The ore mined was smeltered at the mine site, and a very large amount of slag, estimated at 150,000 tons, is scattered there.

Boulders, containing mainly copper ore and a small amount of magnetite and pyrite, scattered around the old mine indicate that the Karadağ mine might have been operated as a copper mine.

A geochemical survey of stream sediment was conducted in the initial phase, and marked geochemical anomalies of Ag, Cu, Mo, Pb, Zn, and W were found in the surveyed area. High anomalies of Pb and Zn indicating five to ten times threshold value were detected especially around Cilaz Mountain. However, the high anomalous area may be caused by contamination from waste rock coming from the old mine. There are no old data or information left on the mine except for the preliminary survey report by MTA and the geochemical survey report by UNDP. At the present time, additional exploration surveys have not been carried out.

1-2 Purpose of the Third Phase Survey

The third survey aimed had the following aims:

- 1) to unravel detailed geology
- 2) to determine distribution of quartz porphyry and graniorite related to mineralization
- 3) to determine characteristics of mineralization in the Karadağ Area (12.0 km²) in which is expected a promising porphyry copper type ore deposit accompanied by a skarn type ore deposit
- 4) to investigate emplacement condition and scale of the ore deposit.

These were accomplished by a comprehensive study together with results of the geophysical survey.

A semi-detailed geological survey and geophysical survey (SIP and IP methods) were performed in the promising ore deposit area extending into limestone, andesite and intrusive stock. As a result, three promising anomalous zones were selected. These anomalous zones were detected as PFE anomalies first by conventional IP survey. A detailed SIP method was performed on these PFE anomalies. The survey result indicates that a promising primary mineralized zone may be present in a deeper zone. The third phase survey aimed to prospect the promising anomalous zones by diamond drilling.

1-3 Survey Methods and Amount of Work

Three anomalous areas regarded as mineralization were found by the geophysical surveys (conventional IP and SIP methods) in the second phase. In the area, an inferred fault striking NE~SW was interpreted through geological surveys, and intrusive rocks have intruded in the structurally weak zone, accompanied by mineralization. A drilling survey (2 holes, 652m in length) was carried out to confirm an ore deposit at the No. 9 point of I-line (MJT-9) and the No.13 point of H-line (MJT-10). The drill locations are shown in Fig.65.

Samples for laboratory tests—namely microscopic observation (rock thin section and ore polished specimen), chemical analysis (Au, Ag, Cu, Mo, Sn, Zn and W), and X ray diffraction analysis—were collected in order to study and clarify characteristics of mineralization and alteration.

Chapter 2 Geology

2-1 General Geology

The geology of the Karadağ Area is divided roughly into Late Paleozoic Gumushane Granite, Lower Cretaceous to Lias Stage Kırıklı Formation, and Upper Cretaceous Zigana Formation. The Zigana Formation is further divided into, five stratigraphic units: Kermutdere, A1, D1, A2, and D2 Members in ascending order. Only the A1 Member (lowest Member of Zigana Formation) is distributed in the survey area. Quartz porphyry, granodiorite and diorite have intruded into the Zigana Formation, and mineralization accompanied by skarnization is embedded at the boundary of the limestone and the andesite of the Zigana Formation. The geological map, geological profile, and schematic geological column are shown respectively in Figs. 62~64.

2-2 Stratigraphy

Gümüşhane Granite : This granite, which is the basement in the area, is widely distributed, stretching in a southwestern direction south of Gümüşhane City. It covers an elliptical area 37 km E-W and 15 km N-S, and the surveyed area is located at this western end of this granite batholith. The granite was dated as 406 Ma by the radiometric Rb-Sr method, indicating intrusion in Early Devonian time.

This rock is generally massive and grayish or yellow white to pink, and its component minerals vary from fine to coarse grained, but the general tendency of

the grain size is to be finer toward the periphery and coarser toward the inner part of the granite. Coarse-grained granite is brittle and consists of quartz 2-3 mm in diameter, and abundant biotite. The aplitic part of the granite is compact, massive, and abundant in quartz, plagioclase and feldspar.

Kırıklı Formation : This formation unconformably overlies the Paleozoic Gümüşhane granite and consists of basaltic lava. Basal conglomerate lies locally at the lowest horizon of the formation, and the basalt lava contains thin intercalated beds of sandstone and mudstone.

Basal conglomerate : This rock is locally distributed and is discontinuous.

It is pale pink in colour and contains mostly granite pebbles, several to tens of centimeters in diameter and rounded to sub-rounded in shape. The matrix is of pale green to grayish white quartz and feldspar grains.

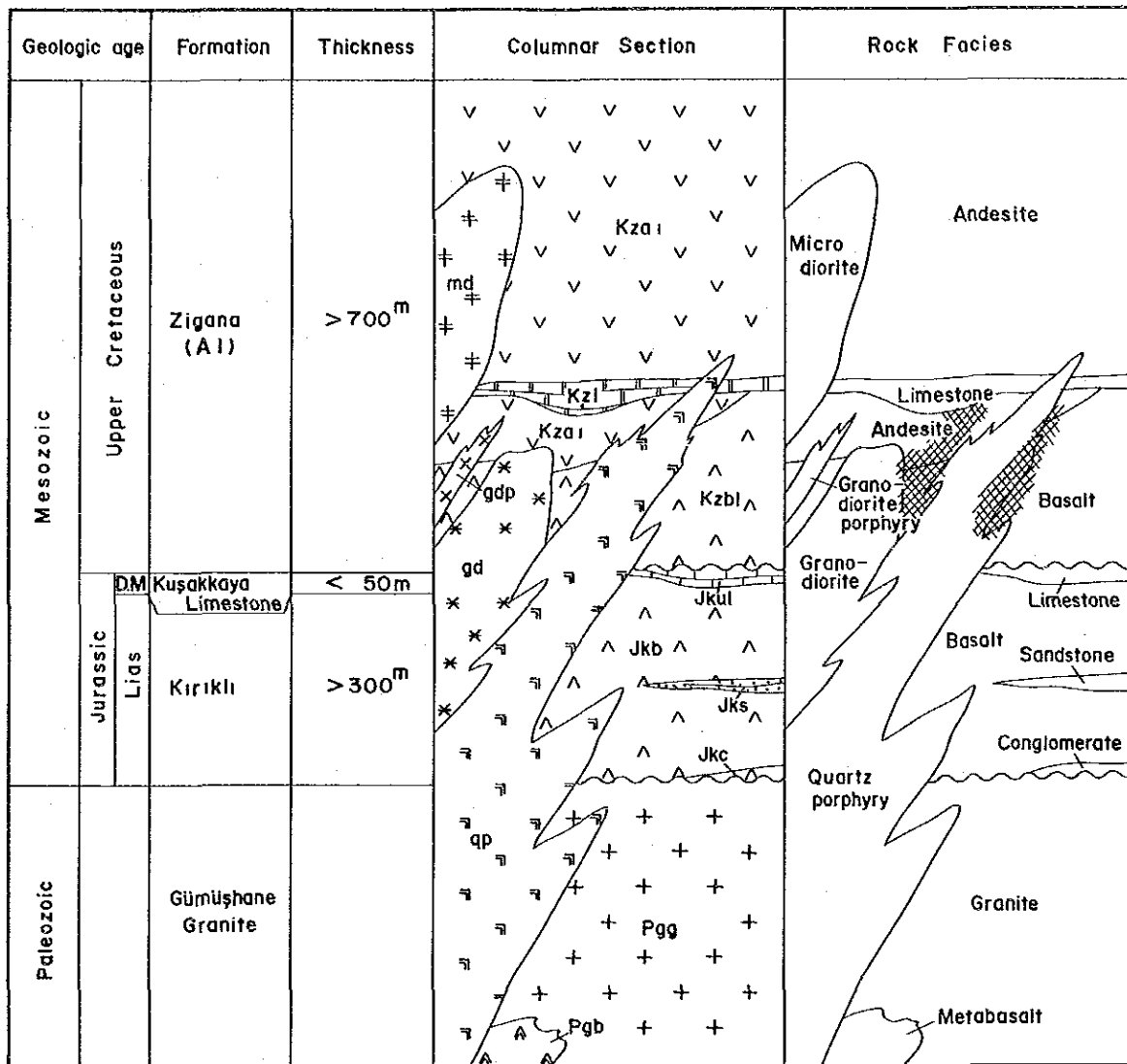
Basalt lava : Basalt lava is generally dark green to reddish brown in colour and has undergone chloritization and epidotization. The lava contains thin intercalated beds of sandstone and mudstone. It unconformably overlies Gümüşhane granite, and is a thin layer on the west side of the granite, while on the east side of the granite, it is a thick layer and widely distributed.

Kuşakkaya Limestone Formation : The formation is distributed in a small square at the north part of the surveyed area. It seems to unconformably overlie the Kırıklı Formation. This rock is massive without bedding, and grayish to white in colour. It is reported that fossils correlating with Dogger and Malm stages of the Upper Jurassic have been discovered at Ucbacalı located approximately 3 km northeast from Altıntaşlar village.

Zigana Formation : This Formation was divided into the Kermutdere, A1, D1, A2, and D2 Members in ascending order by the geological survey of the initial phase.

Only the A1 Member is widely distributed in the Karadağ Area. The A1 Member consists of basaltic lava, and a limestone-sandstone bed. Basalt lava is deposited in the lower horizon and its rock facies gradually changes upward to andesite. Basaltic lava exists in the area from the surveyed area to Avliyana.

The basalt lava is dark green and contains amygdaloidal texture. Phenocrysts of plagioclase and a small amount of pyroxene are observed through the microscope. These phenocrysts are all altered to chlorite, and only the outline of these crystals remain as unaltered rims. The ground mass of the rock has hyalopilitic texture containing lath shaped plagioclase filled with intersertal glass, but most of them have undergone chloritization and calcitization.



D.M : Dogger ~ Maim

Mineralization

Fig. 64 Schematic Geological Column of Karadağ Area

The andesite lava is massive, pale green to dark green in colour, and are partly brecciated. Under microscopic observation, the rock consists characteristically of pyroxene and epidotized plagioclase on the west side of IP survey Line B, whereas hornblende with epidotized and chloritized plagioclase is on the east side of IP Line D.

In the surveyed area, limestone and sandstone beds are intercalated in volcanic rock, and basaltic lava lies at a lower horizon. Andesite lava is in the upper horizon, in contact with the intercalations. The limestone-siltstone, striking N-S with $20^{\circ} \sim 30^{\circ}$ dip, consists of crystalline and massive limestone, black siltstone, and argillaceous mudstone. Limestone exposed at the old Karadağ mine has been crystalized and has undergone skarnitization accompanied with epidote. The south extension of the limestone is dislocated 250 m to the east by a NE-SW fault in the center part of the surveyed area.

2-3 Intrusive Rocks

Intrusive rocks of the Karadağ Area are classified into altered granodiorite, altered quartz porphyry, diorite and granodiorite. These rocks are independently distributed. Thus their intrusion order is not evident. However, it is inferred that the altered granodiorite and quartz porphyry are the older intrusions, and diorite and granodioritic porphyry are younger intrusions.

Altered granodiorite : The rock is exposed up stream of Maden Dere in the central part of the Karadağ Area as a small ellipsoidal stock. The rock divides a limestone bed extending N-S into two parts. Under microscopic observation, it is a hornblende granodiorite consisting of hornblende, plagioclase, and biotite, but these constituent minerals have undergone chloritization and epidotization.

Altered quartz porphyry : The rock is distributed along the west side of the Gümüşhane granite, extending in a NNE-SSW direction. The brecciated part of the intrusion is accompanied by tourmaline, muscovite, and quartz veins. As sulphide ores have been limonitized owing to oxidation on the ground surface, it is difficult to identify the primary sulphide ore. Constituent minerals in the groundmass, except for quartz phenocrysts, have been severely altered to quartz, sericite, epidote and hematite, as observed through the microscope.

Diorite : The intrusive rock outcrops as a stock in the north-east section of the Karadağ Area, forming a hill 800m × 500m in scale. Its microscopic texture is equigranular, and constituent minerals of the rock are albitized plagioclase, and chloritized and epidotized common pyroxene in part.

Granodiorite porphyry : The rock is exposed as a dyke striking NE-SW in the

area on the north-east side of Maden Dere. The rock consists of slightly chloritized plagioclase and hornblende in equigranular texture.

2-4 Geological Structure

The Karadağ Survey Area is situated on the north-west side of Gümüşhane granite which is the basement rock in the area. The Zigana Formation unconformably overlies the Gümüşhane granite, lacking Kırıklı Formation and Kuşakkaya Limestone Formation between both rocks. The rock facies of the Zigana Formation in the area are basalt in the lower horizon and andesite in the upper horizon. A limestone bed with greatly varying thickness is intercalated at the boundary between these two facies and extends south and north.

The limestone bed is divided into two parts by an intrusion of granodiorite in the center part of the surveyed area. A fault striking NE-SW is inferred exist at the intrusion. All intrusive rocks have intruded along the geologically weak zone (inferred fault zone). By tracing the distribution of exposed intrusives and by following their emplacement direction, it is presumed that two parallel weak zones exist.

Chapter 3 Mineralization and Alteration

As mention above, data and information on the old Karadağ Mine are scarce, although an underground mine was operated in ancient times. However, scattered ore blocks around the mine site indicate that the Karadağ ore deposit may contain copper, lead, and zinc ores with a few amounts of magnetite and pyrite. The Karadağ mine probably produced mainly copper.

The Karadağ area is situated in the highlands and its climatic condition is inland type. It is dry, has extreme temperature differences, and in the winter season there is over 3m of heavy snow. These climatic conditions cause severe oxidation of sulphide ores, and primary sulphide ores are barely visible on the surface. X-ray diffraction analysis detected cerucite ($PbCO_3$) which was not identified through naked eye observation.

The samples indicate that copper oxide ore is observed in skarn around the old Karadağ mine site and along Maden Dere. Samples from such places usually contain high grades of copper. The maximum grade among ores collected from around the old Karadağ Mine is 19.8% Cu and 13.50% Zn. Ore from Maden Dere is 14.80% Cu, but has a low zinc grade. Lead content of ore was not chemically analyzed, but some lead can be expected in the ore since lead ore was detected by X ray diffraction analysis.

Based on results of the chemical and X-ray diffraction analyses, the ore

deposits can be classified into two types : copper, lead, and zinc bearing ore deposits around the old Karadağ Mine, and copper ore deposits along Maden Dere.

This is to say that there are two different types of ore deposits in the surveyed area.

Quartz porphyry is characteristically accompanied by tourmaline, muscovite, quartz and limonite. Its groundmass has undergone remarkable sericitization.

The sericite is 2M₁ type and well crystallized, as detected by the X-ray diffraction analysis and by microscopic observation. It is not of hydrothermal mineralization type.

Quartz porphyry and granodiorite may be the ore-bringer intrusions. It is supposed that many fissures are distributed centering around the inferred fault, and that mineralization is emplaced along these fissures.

The mineralization is oxidized on the surface, and limonite ore outcrops on the hill, while pyrite remains only in streams.

Chapter 4 Drilling Survey

4-1 Outline of the Diamond Drilling

(1) Purpose of the Diamond Drilling

As a result of geological, geochemical and geophysical surveys carried out in the initial and second phases of the project, dissemination and contact type mineralizations were expected as a promising target for future exploration in the Karadağ area. In the third phase, a drilling survey consisting of two holes (total hole length 600m) was planned and subsequently carried out in order to explore underground emplacement of the dissemination type ore deposit, and to investigate and unravel the relationship between the emplacement conditions of the ore deposit and the results of the geological, geochemical and geophysical surveys.

The Purpose of these holes are as follows ;

MJT- 9 : Exploration of the IP and SIP anomaly area

MJT-10 : Exploration of the IP and SIP anomaly area

(2) Outline of Drilling Operation

① Location of drill holes

	Y	X	Z [m sea level]
MJT- 9	12 880	67 601	2,382
MJT-10	12 164	67 536	2,386

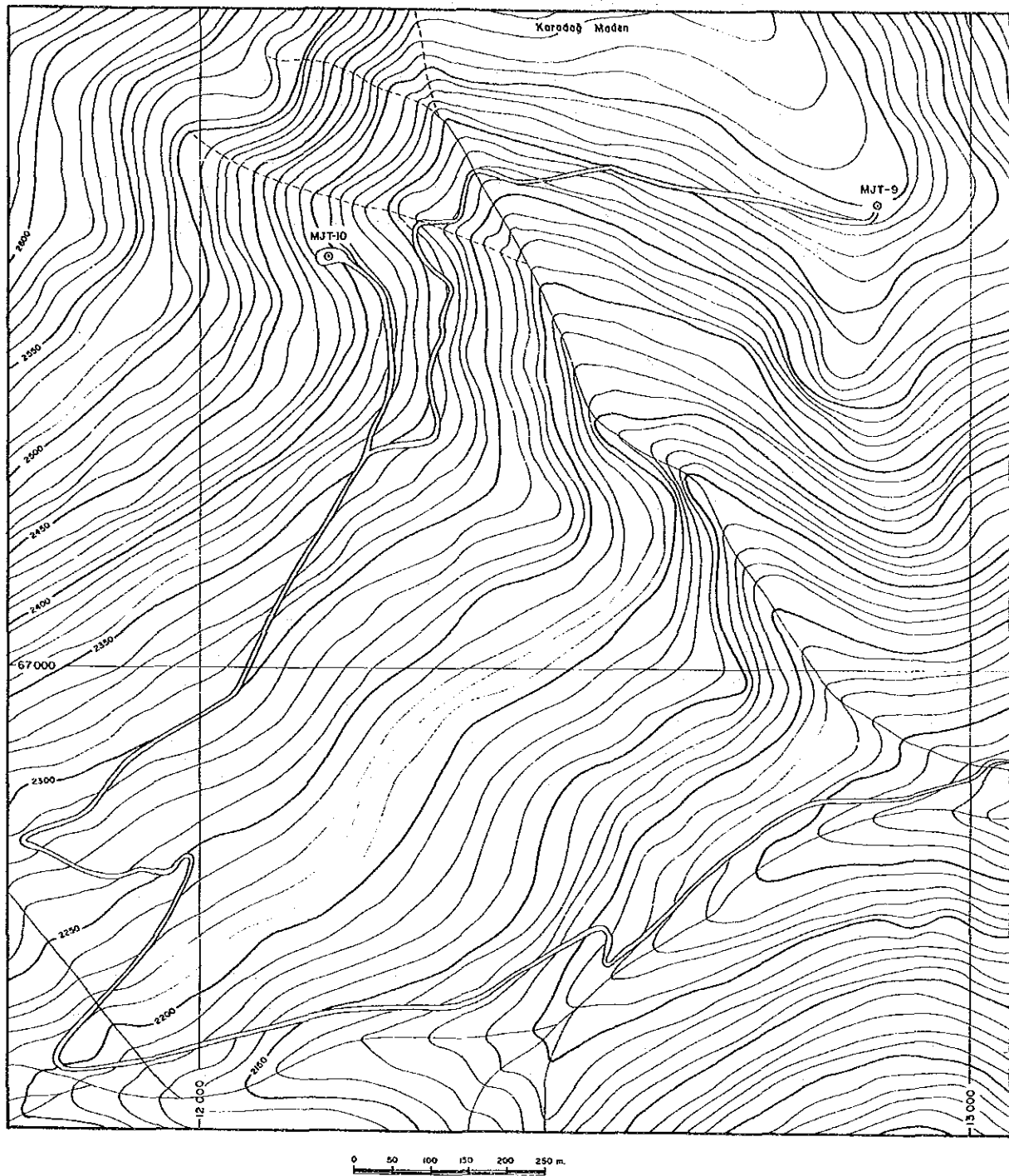


Fig. 65 Location Map of Drill Holes in Karadağ Area

② Drilling operation method

Wire line drilling method using an NQ type diamond bit as far as possible was applied. Drill inclination was vertical.

③ Core survey

A geological columnar section 1/200 in scale was compiled, and colour photographs of all drill cores collected were taken.

④ Chemical assay of drill cores

Mineralized cores were chemically assayed to detect zinc and copper content, while selected samples were analysed for gold, silver, tungsten, tin and molybdenum content.

⑤ Laboratory works on the core

Microscope observations of rock thin sections and ore polished specimens, and detection of altered minerals by X-ray diffraction meter were performed.

(3) Drill Holes Performed

Drill holes were performed as follows;

Drilling No.	Drill length planned	Drill length performed	Dip	Surface soil	Core length	Core recovery	Period
MJT- 9	300m	301.00m	-90°	3.00m	297.60m	98.9%	Aug. 4-Aug. 15
MJI-10	300m	351.00m	-90°	0.70m	328.95m	93.7%	July 7-July 29
Total	600m	652.00m		3.70m	626.55m	96.1%	July 7-Aug. 15

4-2 Drilling Operation

(1) Drilling Method

The drilling operation was performed by means of wire line method as far as possible using a diamond drilling bit of NQ size (75mm diameter). However, the drilling operation was carried out using a diamond bit of BQ size because of the loss of water circulation below 180m. The MJT-9 and MJT-10 sites were covered by surface soil.

Bentonite mud water was circulated during the drilling operation, and cutting oil [lubricant] was suitably added into the circulating mud water in order to reduce torque resistance caused by collapse in the hole.

Geology of the Karadağ area consists of andesite, granodiorite and quartz porphyry. There are many well-developed cracks in the andesite and granodiorite of MJT-9, and also in the limestone of MJT-10. At the

predominantly altered sections of rocks in the holes, the rocks are soft and brittle, and cracks often caused loss of circulating mud water. Strong silicified rock was very hard to drill. Two holes were operated even with the loss of circulating mud water

(2) Drilling Machines and Equipment Used

Acker (capacity: 800m by means of BQ wire line) was used for the drilling operation. Types and specifications of the machine, engine, pump and equipment and amount of consumables are shown in Table 27 and 29.

(3) Operation Members and Shifts

The operation of move-in and move-out from site to site, and preparation work in the site were performed by a shift per day system, while the actual drilling operation was carried out by three shifts per day with eight working hours per shift. One drilling shift consisted of five members: a Japanese drilling engineer, a Turkish driller [MTA] and three Turkish workers.

(4) Transportation and Road Construction

The drilling machines, equipment and consumables were transported from the East Black Sea regional office of MTA located in Trabzon, to a place near these drilling sites by a large truck, and then to the drilling sites by a small truck. As there was no access road to MJT-9 and MJT-10, a new road of 8km was constructed by bulldozer in one month (20 June to 19 July).

(5) Water Supply

The water necessary for the drilling operation was run through a polyetherene pipe line from a neighbouring river.

(6) Withdrawal

After completion of the drilling survey, the drilling machines and equipment were stored in the storehouse of the MTA office in Trabzon. Whole cores were preserved in the MTA camp at Hamsikoy.

4-3 Results of the Diamond Drilling

(1) MJT-9

The hole reached bed rock (andesite) at 3m after cutting through surface soil using an HXSW size diamond bit and circulating dense bentonite mud water. After reaming by the NW casing shoe bit, NW casing pipes were inserted at 3m. Then, the hole reached compact andesite at 6m after cutting by an NQ wire line,

Below 6m, NQ wire line method, libonite mud water and cutting oil were used for the operation. The rock was basaltic andesite and drilling continued to 180m, where BX casing pipes were inserted because of well-developed cracks. Below 180m, the drilling operation was carried out by the BQ wire line method, circulating libonite mud water and cutting oil. The rock was altered granodiorite; the hole lost water circulation at 239.85m. The drilling was continued using bentonite, and completed at 301.00m.

Depth (m)	0~3.00	3.00~6.00	6.00~180	180~301.00
Mud Water	Bentonite mud water		Libonite mud water Cutting oil	
Bit Exchange (pcs)	HXSW(1)	NQWL bit(1)	NQWL bit(5)	BQWL bit(3)
Pump Pre. (kg/cm ²)	3	3	3~10	0~18
Pump Feed (ℓ/min)	60~70	50~60	50~60	50
Pump deri (ℓ/min)	60~70	50~60	50~60	0~30
Bit Pre. (kg/cm ²)	800~1,000		800~1,200	800~1,000
Bit Rot. (rpm)	200~250		250~300	250~300
Core Recovery (%)	20	67	100	100

(2) MJT-10

The hole reached bed rock (weathered granodiorite) at 3.10m after cutting through surface soil using an HXSW size diamond bit and circulating dense bentonite mud water. After reaming by the NW casing shoe bit, NW casing pipes were inserted at 3.10m. Then, the hole reached compact granodiorite at 7.40m after cutting by an NQ wire line. Below 7.40m, NQ wire line method, libonite mud water and cutting oil were used for the operation. The rock consisted mainly of limestone, altered granodiorite and andesite. Drilling was continued to 180m, where BX casing pipes were inserted at 180m because of loss of water circulation. Below 180m, the drilling operation was carried out by a BQ wire line method, circulating libonite mud water and cutting oil. The whole rock was limestone. The drilling operation continued to remain as it was with loss of water circulation after insertion of the BW casing pipes. The drill hole was extended to 351.00m because mineralization was not intersected until 300.00m. The hole was completed at 351m.

Table 27 Drilling Machine and Equipment Used (Karadağ Area)

<u>Drilling Machine Model " acker "</u> Specifications : Capacity Dimensions L × W × H Hoisting capacity Spindle speed Engine Model " F4L912 "	1 set 800 m (BQ - WL) 2,310mm × 1,070mm × 1,650 6,795 kg Forward 232,481,880,1,484 rpm 18 ps / 1,800 rpm
<u>Drilling Pump Model " 535 RQ "</u> Specifications : Piston diameter Stroke Capacity Dimensions L × W × H Engine Model " WISCON "	1 set 70 mm 70 mm Discharge capacity 132 l/min Max pressure 56 kg/cm ² 1,905mm × 788mm × 940mm 18ps / 2,000 rpm
Wire line hoist	Attached to drilling machine
Derick	Attached to drilling machine
<u>Drilling tools</u> Drilling rod Casing pipe	NQ - WL 3 m 70 pcs BQ - WL 3 m 150 pcs HW 1.5 m 4 pcs NW 3 m 30 pcs BW 3 m 70 pcs

Table 28 Drilling Meterage of Diamond Bit Used (Karadağ Area)

Item	Size	Drilling Meterage by Unit						
		MJT-9			MJT-10			
		No.	m	m/pc	No.	m	m/pc	
Bit	HX	HXSW	3.00		HXSW	3.10		
		NN-64	30.65		NN-59	23.45		
	NQ	NN-65	35.90		NN-60	55.15		
		NN-66	59.75		NN-61	25.20		
		NN-67	34.55		NN-62	22.45		
		NN-68	16.15	35.40	NN-63	50.65		38.38
BQ	175811	35.75		175812	28.55			
	175813	54.05		175815	36.50			
	157810	31.20		175816	55.95			
			40.33	175820	50.00		42.75	
Reamer	HX	HXSW	3.00		HXSW	3.10		
		R-10	66.55		R-1	78.60		
		R-11	59.75		R-2	47.65		
BQ	R-12	50.70		R-3	50.65			
			59.00				58.97	
	375151	89.80		375148	65.05			
Casing shoe bit (NW)	A-12139	375152	31.20		375149	55.95		
				60.50	375150	50.00		57.00
		A-12139	6.00		A-12189	7.40		

Table 29 List of Consumables Used (Karadağ Area)

Description	Specification	Unit	Quantity		
			MJT-9	MJT-10	Total
Light oil		ℓ	2,580	2,780	5,360
Petrol		ℓ	1,780	2,190	3,970
Engine oil		ℓ	50	85	135
Hydraulic oil		ℓ	30	67	97
Grease		Kg	4	9	13
Cement		Kg	1,500	1,500	3,000
Bentonite		T	4.75	12	16.75
C.M.C		Kg	113	150	263
Cutting oil		ℓ	140	400	540
Tel stop		Kg	35	140	175
Diamond bit	HX	pcs	1	1	2
Diamond reamer	HX	pcs	1	1	2
Diamond bit	NQ/BQ	pcs	5/4	5/4	10/8
Diamond reamer	NQ/BQ	pcs	3/2	3/3	6/5
Casing diamond shoe	NW/BW	pcs	1/0	1/1	2/1
Casing metal shoe	HX/BW	pcs	1/1	1/0	2/1
Core barrel Ass'y	NQ/BQ	set	2/2	2/2	4/4
Inner tube	NQ/BQ	pcs	3/3	3/3	6/6
Core lifter case	NQ/BQ	pcs	5/5	5/5	10/10
Core lifter	NQ/BQ	pcs	6/6	8/7	14/13
Thrust ball bearing	NQ/BQ	pcs	5/5	6/4	11/9
Chack piece	NQ/BQL	set	1/1	2/1	3/2
Cylinder liner	535-RQ	pcs	1	1	2
Valve seat	535-RQ	pcs	1	1	2
Steel ball	535-RQ	pcs	1	1	2
Piston rubber	535-RQ	pcs	2	2	4
Core box	NQ	pcs	57	60	117

Table 30 Working Time Table of the Drilling Operation (Karadağ Area)

Hole-No	Drilling		Shift		Working man							Working Time				
	Bit size	Drilling length m	Core m	Drilling shift	Total shift	Engineer man	Worker man	Drilling h	Other working ring h	Recover- ring h	Total h	Removing working h	Water traspor- tation h	Road con- struction and others h	G.Total	
MJT- 9	HX	3.00	0.60	1	1	3	4	1.00	3.00		4.00				4.00	
	NQ	177.00	176.00	16	17	16	64	86.50	37.10		124.00				124.00	
	BQ	121.00	121.00	15	32	15	60	53.00	67.00		120.00				120.00	
Total		301.00	297.60	32	32	34	128	140.50	107.10		248.00				248.00	
MJT-10	HX	3.10	1.00	1	1	3	5	4.00	4.00	-	8.00				8.00	
	NQ	176.90	160.85	32	33	37	128	104.30	141.40	10.00	256.00				264.00	
	BQ	171.00	167.10	22	55	23	88	63.40	112.20	-	176.00				440.00	
Total		351.00	328.95	55	55	63	221	172.00	258.00	10.00	440.00				440.00	
G. total		652.00	626.55	87	87	97	349	312.50	365.10	10.00	688.00				688.00	

Table 31 Record of the Drilling Operation of MJT-9

	Drilling length			Total		Shift		Working man	
	Shift.1 m	Shift.2 m	Shift.3 m	Drilling m	Core length m	Drilling shift	Total shift	Engineer man	Worker man
26 July	Pds						1	3	8
27 July	Pds						2	3	10
1 Aug.	Pds						3	3	10
2 Aug.	Pds						4	3	10
3 Aug.	Pds						5	3	10
4 Aug.	6.40			6.40	3.00	1	6	3	10
5 Aug.	6.80	10.05	10.40	33.65	30.25	3	9	3	10
6 Aug.	11.55	12.20	12.15	69.55	66.15	3	12	3	10
7 Aug.	12.60	11.45	12.30	105.90	102.50	3	15	3	10
8 Aug.	12.20	11.20	11.80	141.10	137.70	3	18	3	12
9 Aug.	12.20	10.55	10.50	174.35	170.95	3	21	3	12
10 Aug.	5.65	Ins C.P	5.25	185.25	181.85	3	24	3	12
11 Aug.	9.15	12.20	9.15	215.75	213.35	3	27	3	12
12 Aug.	6.10	12.05	8.45	242.35	238.95	3	30	3	12
13 Aug.	9.15	9.15	9.15	269.80	266.40	3	33	3	12
14 Aug.	6.10	12.15	9.15	297.20	293.80	3	36	3	10
15 Aug.	3.80	Out-C.P		301.00	297.60	2	38	3	10
16 Aug.	Dismant						39	3	10
17 Aug.	Tra-Ress						40	3	10
18 Aug.	Tra-Ress						41	3	10
19 Aug.	Tra-Ress						42	3	5
Total	101.70	101.00	98.30	301.00	297.60	33	42	63	215

Abbreviation

Road-con ; Road-construction

Pds ; Preparation for drilling site

Transpor ; Transportation

Tra-Ress ; Transportation and Reassemblage

Dismant ; Dismantlement

Reco ; Recovering work

Ins-C.P ; Inserting casing pipe

Out-C.P ; Taking out casing pipe

Table 32 Record of the Drilling Operation of MJT-10

	Drilling length			Total		Shift		Working man	
	Shift.1 m	Shift.2 m	Shift.3 m	Drilling m	Core length m	Drilling shift	Total shift	Engineer man	Worker man
2 July	Pds						1	3	8
3 July	Pds						2	3	8
4 July	Pds						3	3	8
5 July	Pds						4	3	8
6 July	Pds						5	3	6
7 July	3.10			3.10	1.00	1	6	3	6
8 July	4.80			7.90	3.30	1	7	3	8
9 July	2.80			10.70	4.40	1	8	3	8
10 July	6.55	5.90	2.60	25.75	15.10	3	11	3	8
11 July	O.W	Reco				2	13	3	8
12 July	O.W	0.80	12.20	38.75	28.10	3	16	3	8
13 July	10.40	5.05	7.95	62.15	45.80	3	19	3	10
14 July	11.00	7.70	0.85	81.70	64.15	3	22	3	12
15 July	O.W	11.85	11.50	105.05	87.50	3	25	3	12
16 July	1.85	9.35	2.65	118.90	101.35	3	28	3	12
17 July	O.W	8.45	2.00	129.35	111.55	3	31	3	12
18 July	O.W	8.30	9.35	147.00	128.85	3	34	3	12
19 July	8.80	10.00	11.55	177.35	159.00	3	37	3	12
20 July	2.65	Ins-C.P	6.95	186.95	167.30	3	40	3	12
21 July	10.55	8.05	3.00	208.55	187.95	3	43	3	12
22 July	O.W	1.25	5.25	215.05	194.05	3	46	3	12
23 July	11.80	9.85	8.35	245.05	223.00	3	49	3	12
24 July	11.20	10.25	13.55	280.05	258.00	3	52	3	10
25 July	14.70	6.25	-	301.00	278.95	2	54	3	10
26 July	※								
27 July	※								
28 July	O.W	12.05	11.35	324.40	302.35	3	57	3	12
29 July	12.20	12.30	2.10	351.00	328.95	3	60	3	12
30 July	Out-C.P						61	3	10
31 July	Dismant						62	3	10
Total	112.40	127.40	111.20	351.00	328.95	56	62	84	278

Abbreviation

Road-con ; Road-construction

Pds ; Preparation for drilling site

Transpor ; Transportation

Tra-Ress ; Transportation and Reassemblage

O.W ; Other working

Dismant ; Dismantlement

Reco ; Recovering work

Ins-C.P ; Inserting casing pipe

Out-C.P ; Taking out casing pipe

※ ; Preparation for MJT-9

Table 33 Summary of the Drilling Operation of MJT-9.

	Survey Period				Total man day		
	Period	Days	Work day	Off day	Engineer	Worker	
Operation	26 July ~ 27 July		days	days	man	man	
Preparation	1 August ~ 3 August	5	5	-	15	48	
Drilling	4 August ~ 15 August	12	Drilling				
			12	-	36	132	
Recovering							
Removing	16 August ~ 19 August	4	4	-	12	35	
Total	26 July ~ 19 August	21	21	-	63	215	
Drilling length	Core recovery of 100 m hole						
Length planned	300.00m	Overburden	3.00m	Depth of hole	Core recovery	Core recovery cumulated	
Increase or Decrease in length	m	Core length	m	(m)	(%)	(%)	
Length drilled	301.00m	Core recovery	297.60	0 ~ 100	96.6	96.6	
			98.9	100 ~ 200	100.0	98.3	
				200 ~ 301	100.0	98.9	
Working hours	h	%	%	Efficiency of Drilling			
Drilling	140.50	53.3	41.9	Total m/work period(m/day)	301.00m/21 days (14.33m/day)		
Other working	123.10	46.7	36.7	Total m/total shift (m/shift)	301.00m/42 shifts (7.17m/shift)		
Recovering				Drilling length/bit(each sized bit)			
Total	260.00	100	78.6	Bit size	HX	NQ	BQ
Reassemblage	40.00		8.1	Drilled length	3.00	177.00m	121.00m
Dismantlement	32.00		9.5	Core length	0.60	176.00m	121.00m
Water transportation							
Road construction and others							
G.Total	336.00		100				
Casing pipe inserted							
Size	Meterage (m)	Meterage drilling length (%)	Recovery (%)				
HX	3.0	1.0	100				
NW	6.0	2.0	100				
BW	180	59.8	100				

Table 34 Summary of the Drilling Operation of MJT-10

Operation	Survey Period				Total man day		
	Period	Days	Work day	Off day	Engineer	Worker	
			days	days	man	man	
Preparation	2 July~ 6 July	5	5	-	15	37	
Drilling	7 June~25 July	21	Drilling	-	63	221	
	28 July~29 July		Recovering				
Removing	30 July~31 July	2	2	-	6	20	
Total	2 June~31 July	28	28	-	84	278	
Drilling length			Core recovery of 100 m hole				
Length planed	300.00m	Overburden	3.10m	Depth of hole (m)	Core recovery (%)	Core recovery cumulated (%)	
Increase or Decrease in length	50.00m	Core length	328.95m				
Length drilled	351.00m	Core recovery	93.7 %	0 ~ 100	82.3	82.3	
				100 ~ 200	97.2	89.9	
				200 ~ 300	98.6	92.8	
				300 ~ 351	100	93.7	
Working hours	h	%	%	Efficiency of Drilling			
Drilling	185.50	42.2	37.5	Total m/work period(m/day)		351.00m/28 days	
Other working	244.10	55.5	49.2	(12.54m/day)			
Recovering	10.00	2.3	2.0	Total m/total shift (m/shift)		351.00m/62 shifts	
Total	440.00	100	88.7	(5.66m/shift)			
Reassemblage	40.00		8.1	Drilling length/bit(each sized bit)			
Dismantlement	16.00		3.2	Bit size	HX	NQ	BQ
Water transportation				Drilled length	3.10	176.90m	171.00m
Road construction and others				Core length	1.00	160.85m	167.10m
G.Total	496.00		100				
Casing pipe inserted	Meterage		Recovery				
Size	Meterage (m)	Meterage drilling × 100 length (%)		(%)			
HX	3.1	0.9	100				
NW	7.4	2.1	100				
BW	180	51.3	100				

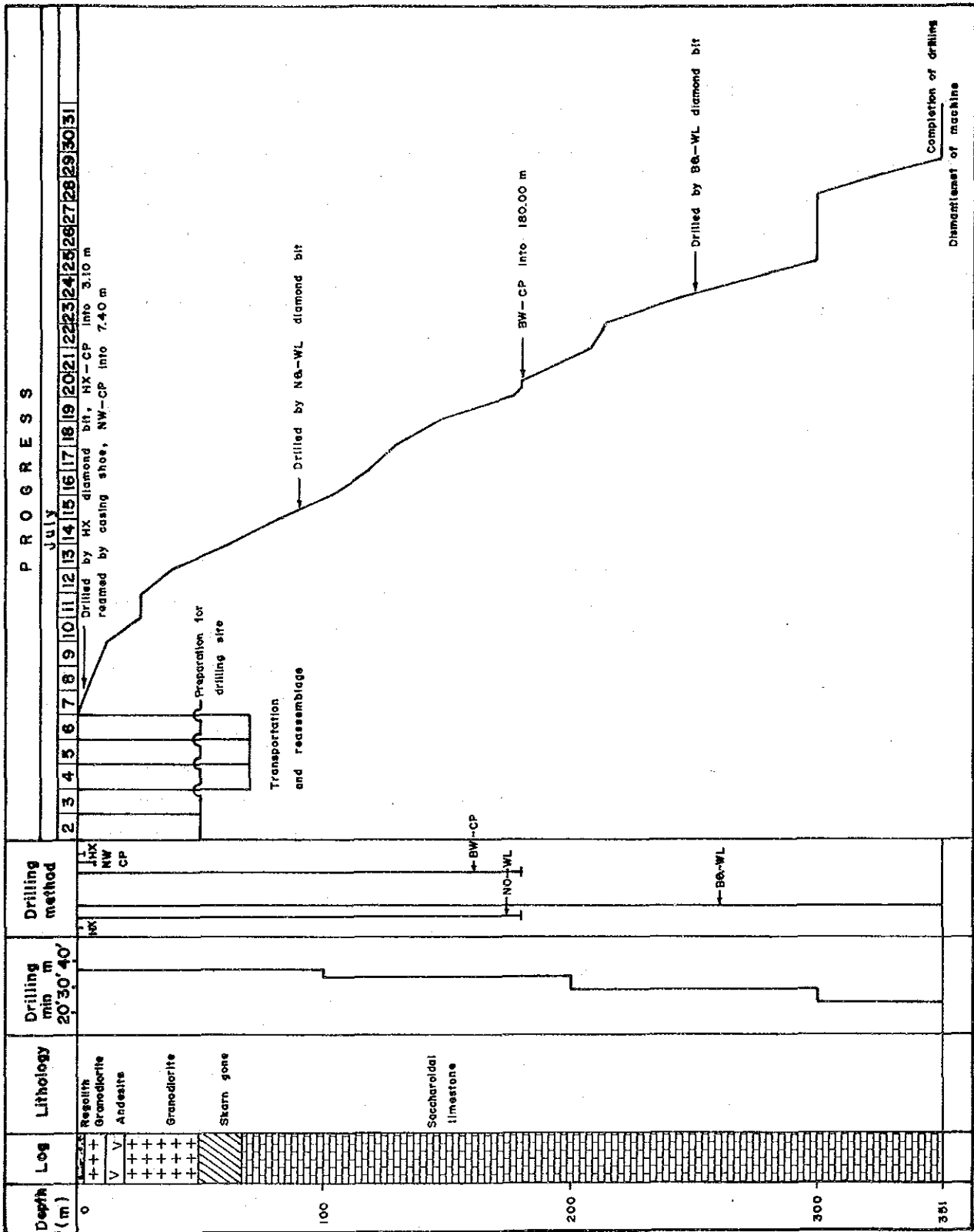


Fig. 67 Drilling Progress of MJT-10